Synthesis and Application of [Zr-UiO-66-PDC-SO3H]Cl MOFs at The Preparation of Dicyanomethylene Pyridines via Chemical and Electrochemical Methods

Amir Mohammad Naseri
Bu-Ali-Sina University

Mahmoud Zarei
Bu-Ali-Sina University

Saber Alizadeh
Bu-Ali-Sina University

Saeed Babaee
Bu-Ali-Sina University

Mohammad Ali Zolfigol
Bu-Ali-Sina University

Davood Nematollahi (✉ nemat@basu.ac.ir)
Bu-Ali-Sina University

Jalal Arjomandi
Bu-Ali-Sina University

Hu Shi
Shanxi University

Research Article

Synthesis and application of [Zr-UiO-66-PDC-SO₃H]Cl MOFs at the preparation of dicyanomethylene pyridines via chemical and electrochemical methods

Amir Mohammad Naseri[1], Mahmoud Zarei[1*], Saber Alizadeh[1*], Saeed Babaee[1], Mohammad Ali Zolfigol[1*], Davood Nematollahi[1*], Jalal Arjomandi[1], & Hu Shib[2]

[1]Faculty of Chemistry, Bu-Ali-Sina University, Hamedan 65174-38683, Iran. [2]School of Chemistry and Chemical Engineering, Institute of Molecular Science, Shanxi University, Taiyuan 030006, China. *email: mahmoud8103@yahoo.com; s.alizadeh93@basu.ac.ir; zolfi@basu.ac.ir; nemat@basu.ac.ir

ABSTRACT

A metal-organic frameworks (MOFs) with sulfonic acid tags as a novel mesoporous catalyst was synthesized. The precursor of Zr-UiO-66-PDC was synthesized both via chemical and electrochemical methods. Then, zirconium based mesoporous metal-organic framework [Zr-UiO-66-PDC-SO₃H]Cl was prepared by reaction of Zr-UiO-66-PDC and SO₃HCl. The structure of [Zr-UiO-66-PDC-SO₃H]Cl was confirmed by FE-SEM and TEM. This mesoporous [Zr-UiO-66-PDC-SO₃H]Cl was successfully applied for synthesis of dicyanomethylene pyridine derivatives *via* condensation of various aldehyde, 2-aminoprop-1-ene-1,1,3-tricarbonitrile and malononitrile. At the electrochemical section, a green electrochemical method has successfully employed for rapid synthesis of the zirconium based mesoporous metal-organic framework UiO-66-PDC at room temperature and atmospheric pressure. The synthesized UiO-66-PDC has a uniform cauliflower-like structure with 13.5 nm mean pore diameter and 181.6 m² g⁻¹ surface area. The described catalyst [Zr-UiO-66-PDC-SO₃H]Cl was also employed for the convergent paired electrochemical synthesis of dihydropyridine derivatives as an environmental friendly technique under constant current at 1.0 mA cm⁻² in an undivided cell. The proposed method proceeds with moderate to good yields for the model *via* a cooperative vinylogous anomeric based oxidation.

Introduction

28 Functionalized metal-organic frameworks (MOFs) are crystalline structures composed from suitable organic

29 ligands and metal centers.[1] So far, these materials have been applied such as catalyst, [2] adsorbents and so on.[3-4]

30 Ionic liquids-like MOFs (IL@MOFs) as a novel homolog porous materials are some useful properties such as

31 nonflammability, high thermal and chemical stability. Therefore, joining of ionic liquids (ILs) and metal-organic

32 frameworks (MOFs) as novel materials have been used as catalysts, gas adsorption and reagents.[5,6] This strategy

33 have been modified adjust to physical or chemical properties, pore size, surface area, topology, and polarity of

34 IL@MOFs by suitable choice of metal, ligands and other moieties.

35   Zirconium is widespread in nature and used in biological systems. Firstly Zr-based metal-organic

36 frameworks (Zr-MOFs) by Lillerud *et al.* in 2008 was prepared and reported[7]. Zr-MOFs has higher thermal

37 stability and outstanding chemical stability in solvent and air[8] than other M-MOFs (M = metal) which made

38 them applicable for industrial process and organic synthesis. Topology or morphology of Zr-MOFs are such as

39 Fcu, Csq, Ftw, Bct, Spn, Sqc and etc [9-12] Topology of Zr-UiO-66-PDC as one of the precursors for the preparation

40 of the presented [Zr-UiO-66-PDC-SO$_3$H]Cl have been studied.[13]

41   Ionic liquids with N-S bonds has been introduced by Zolfigol *et al.* in 2011.[14] These materials have been

42 applied as catalysts, reagents and solvents in synthesis of wide range of organic compound. [15,16] In 2013, 1-

43 sulfopyridinium chloride [pyridine-SO$_3$H]Cl has been synthesized by reaction of chlorosulfonic acid and

44 pyridine (1:1) at 0 ºC, which have been applied for synthesis of other ILs with other anions via anion exchange

45 methods.[15-18] To combined of metal-organic frameworks (MOFs) and ionic liquids (ILs), we have reacted Zr-

46 UiO-66-PDC and ClSO$_3$H for preparing [Zr-UiO-66-PDC-SO$_3$H]Cl as a novel porous catalyst.

2

47   In recent years, many efforts have been made to investigate the biological properties pyridine and its

48   derivatives. Therefore, it is very important to provide novel and easy strategies for the synthesis of target

49   molecules with specific properties. In this regard, pyridines and 1,4-dihydropyridines are suitable candidates for

50   biological and pharmacological studies. [19,20] These compounds have been applied as drugs for cancer, malaria,

51   HIV, antimicrobial, anti-tumor, antifungal, anticonvulsant, antihypertension and urinary incontinence treatment.

52   [19-27]

53   On the other hand, the chemical reactivity is very complex. Numerous factors control the reaction

54   mechanisms which are subject of everyday experiences. According to the alabugin's theory, one of the most

55   effective factors is stereoelectronic effects, which are the stabilizing interactions of orbitals in space, are based

56   on the quantum nature of molecular bonding but express this nature in a set of simple and intuitive practical

57   rules that build a bridge between structure and reactivity [28,29] Anomeric effect (AE) has been divided to different

58   kinds such as germinal (Endo, Exo and reverse), vinylogous and so on (Figure 1, Part I).[28]

59   The relationship and detail the impact of AE as an oldest tereoelectronic effect on structure and reactivity is

60   also our main interest. This paper attempts to describe the role of vinylogous AE in the course of synthesis of

61   target molecules**.** Recently, we have introduced and developed a new term entitled "anomeric based oxidation"

62   (ABO) in the course of special reactions.[32-38]. Cooperative gaminal and vinylogous ABO has been reviewed

63   (Figure 1, Parts II and III).[30,31] Behind the chemical studies, many efforts have been done to access a mild and

64   green condition for the electrosynthesis and application of MOFs [39-50]. Anodic and cathodic electrosynthesis

65   methods are the important techniques that recently have been used for the preparation of various kinds of

66   MOFs[39-44]. Even though the significant chemical[51-53] and electrochemical synthesis[54-56] of Zr based MOFs have

67   been dedicated to the UiO-66 MOF, there is no any reports using cathodic electrosynthesis of UiO-66 derivatives

68   at room temperature and pressure.

69   In this work, we wish to report the electrosynthesis of the mesoporous UiO-66-PDC (Zr-mMOF) via a

70   reductive electrosynthesis technique as the first example. It was found that the electrosynthesis of Zr-mMOF by

3

71   this method is rapid and could be done at the room temperature and pressure without the need to any base or pre-

72   base additive for activation of the ligand.
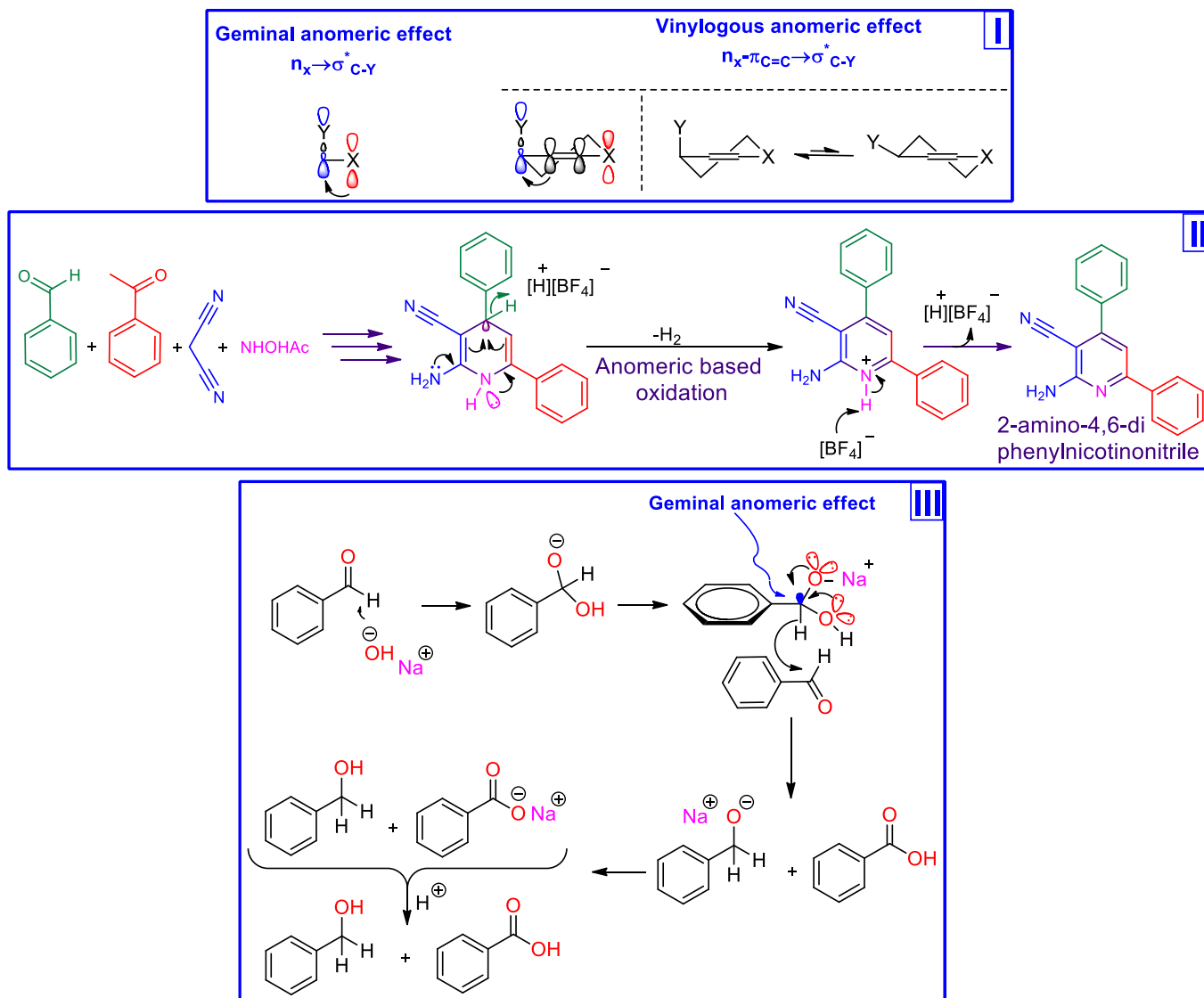
73

Figure 1. Part I: Geminal versus vinylogous anomeric effect. Part II: A cooperative vinylogous anomeric based oxidation leads to the preparation of 2-amino-4,6-diphenylnicotinonitrile [30]. Part III: A cooperative germinal anomeric based oxidation leads to hydride transfer in the mechanism of Cannizzaro reaction [31] (CambridgeSoft).

This results proved by the Fourier Transforms Infrared (FT-IR) spectroscopy, Field Emission Scanning Electron Microscopy (FE-SEM) and N_2 adsorption-desorption isotherm. At the second step and after treatment of electro-synthesized UiO-66-PDC by the SO_3HCl, the catalyst, [Zr-UiO-66-PDC-SO_3H]Cl was employed in

4

80   an green procedure for convergent paired electrosynthesis of dihydropyridine compounds. "Paired

81   electrosynthesis" have been successfully employed for the synthesis of organic and inorganic compounds.[40,57-59]

82   This positive glance comes from the improved energy efficiency, enhanced atom economy, time-saving, and

83   increasing electrochemical yield.[60-63] We imagined that the convergent pairing of two electrochemical reactions

84   would provide a promising protocol towards the green chemistry principles. In other words, by the

85   implementation of this strategy, cooperative anodic and cathodic reactions lead to a one-step process at green

86   solvent and room temperature and without the need for any ex-situ base additive and replacement of the

87   electrodes.

88   According to the above concepts, after preparation of Zr-metal-organic frameworks [Zr-UiO-66-PDC-

89   SO₃H]Cl as a mesoporous catalyst, it was employed for the synthesis and electrosynthesis of special

90   dicyanomethylene pyridines by condensation of various aldehydes (bearing electron-donating and electron-

91   withdrawing groups), malononitrile and 2-aminoprop-1-ene-1,1,3-tricarbonitrile under solvent-free conditions

92   at 100 °C (method A) and constant current electrolysis via the convergent paired electrosynthesis in the ethanol

93   at room temperature and pressure (method B) (Figure 2).
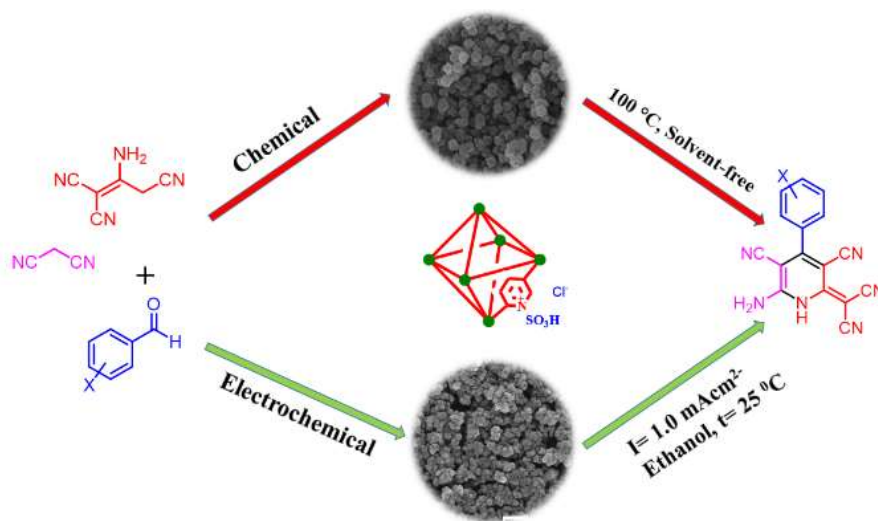
94

95   **Figure 2.** Synthesis of dicyanomethylene pyridines using [Zr-UiO-66-PDC-SO₃H]Cl as a catalyst by chemical and

96   electrochemical methods.

97   **Results and Discussion**

5

98 Nowadays inter and multidisciplinary researches and investigations are a great demand both for academics and

99 industries researchers. On the other hand, making bridges between basic to advanced concepts are necessary for

100 development knowledge. In this research, chemical and electrochemical methods for preparation designed molecules

101 were applied. Stereoelectronic effects a bridge between structure and reactivity was also considered in the course of

102 reactions [28] With this aim, we have studied reactions and the obtained results are presented.

103 **Chemical and electrochemical preparation of Zr-mMOF.** Metal-organic frameworks (MOFs) based on Zr is

104 attractive groups for preparing catalysts and/or reagents. Herein, we attempt to preparation of Zr-UiO-66-PDC with

105 sulfonic acid groups. For this propose, we prepared Zr-UiO-66-PDC *via* H_2PDC and $ZrCl_4$ [13]. Then, [Zr-UiO-66-

106 PDC-SO_3H]Cl was prepared as ionic liquid transported into Zr-UiO-66-PDC. The structure of mentioned ionic liquid

107 transported into Zr-MOFs, [Zr-UiO-66-PDC-SO_3H]Cl, fully was characterized by applying FT-IR, XRD, BET/BJH,

108 TG, DTG, EDX, SEM as well as TEM analysis.

109 The FT-IR spectrum of pyridine-2,5-dicarboxylic acid (H_2PDC), $ZrCl_4$, Zr-UiO-66-PDC and [Zr-UiO-66-PDC-

110 SO_3H]Cl were compared in Figure 3. The broad peak of O-H stretching related to SO_3H group at 2700-3500 cm^{-1} and

111 peaks observed at 1222-1002 cm^{-1} were related to stretching O-S and N-S respectively. The peak 1733 cm^{-1} in H_2PDC

112 was related to stretching C=O bond.

113 The materials in the structure of [Zr-UiO-66-PDC-SO_3H]Cl and Zr-UiO-66-PDC were characterized by energy

114 dispersive X-ray spectroscopy (EDX) (Figure 4). The [Zr-UiO-66-PDC-SO_3H]Cl was confirmed the existence of Zr,

115 C, O, S, Cl and N atoms whereas the structure of Zr-UiO-66-PDC which is contained Zr, C, N and O atoms.

116 Furthermore, well-dispersed of material in the [Zr-UiO-66-PDC-SO_3H]Cl was determined and verified by SEM-

117 elemental mapping (Figure 4). The difference between FT-IR, EDX and SEM-elemental mapping of Zr-UiO-66-PDC

118 and [Zr-UiO-66-PDC-SO_3H]Cl vouched the structure of target Zr-MOFs.
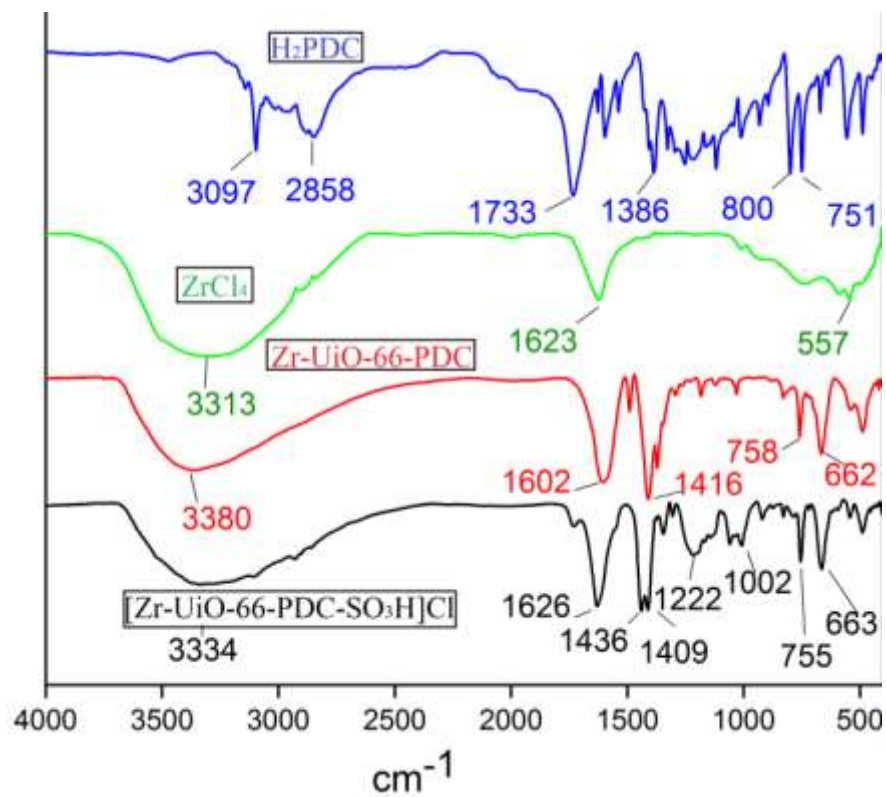
119

120   **Figure 3.** FT-IR spectrum of pyridine-2,5-dicarboxylic acid (H₂PDC), ZrCl₄, Zr-UiO-66-PDC and [Zr-UiO-66-PDC-
121   SO₃H]Cl.

122

7

123
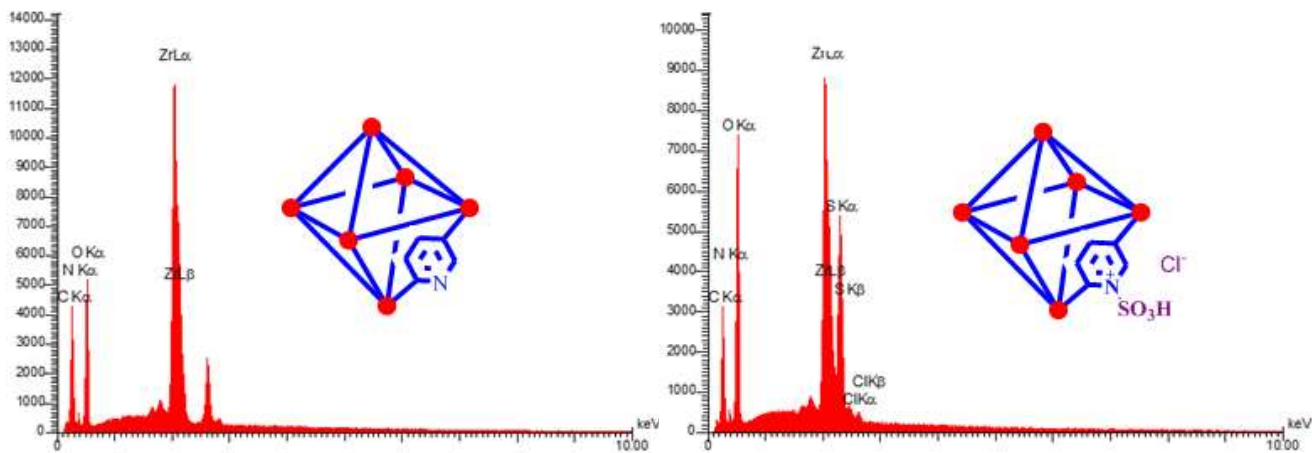
Figure 4. Up: Energy-dispersive X-ray spectroscopy (EDX) of [Zr-UiO-66-PDC-SO$_3$H]Cl and Zr-UiO-66-PDC.

Down: Elemental mapping analysis of [Zr-UiO-66-PDC-SO$_3$H]Cl. The structures of the compounds were drawn

using ChemOffice 12.0 (CambridgeSoft).

127   In another investigation, topography of [Zr-UiO-66-PDC-SO$_3$H]Cl was examined by scanning electron

128   microscopy (SEM) images. As shown in Figure 5, topography particles of the catalysts are Fcu which are in a good

129   agreement and not completely accumulated. In addition, topography structure of [Zr-UiO-66-PDC-SO$_3$H]Cl was

130   studied more closely using transmission electron microscopy (TEM) micrograph in Figure 5. Therefore, [Zr-UiO-66-

131   PDC-SO$_3$H]Cl are fcu topological network with 12-connected Zr clusters.
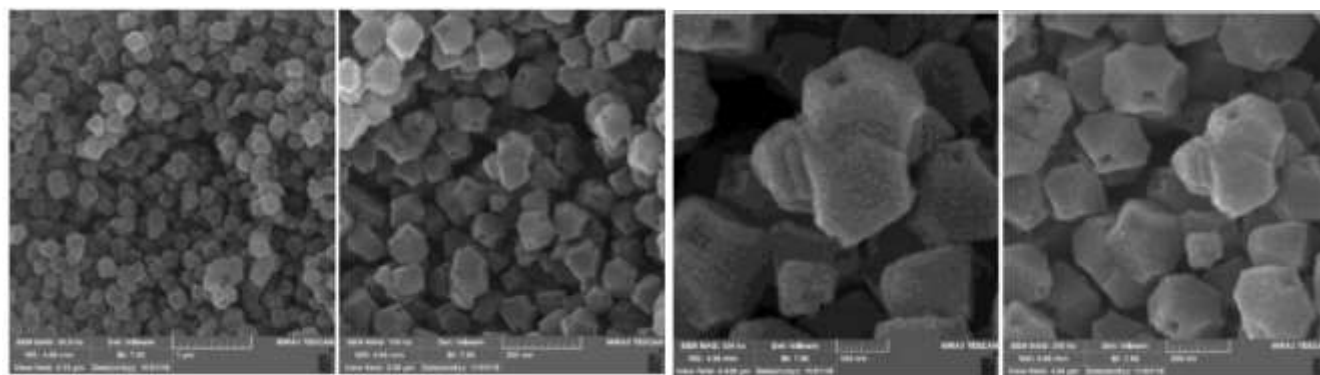

132
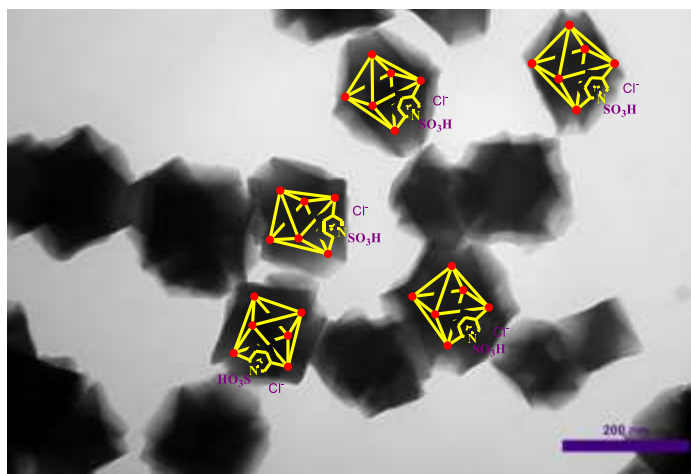
8

Figure 5. Up: Scanning electron microscopy (SEM) images of [Zr-UiO-66-PDC-SO3H]Cl. Down: Transmission electron microscopy (TEM) micrograph of [Zr-UiO-66-PDC-SO$_3$H]Cl.

In order investigation, structural and thermal stability of [Zr-UiO-66-PDC-SO$_3$H]Cl was also determined using technique of the thermal gravimetric (TG), derivative thermal gravimetric (DTG), as well as the differential thermal analysis (DTA) (Figure 6). Initial stage weight losing is between room temperature up to 100 °C, associated with organic solvents and H$_2$O which have been applied in the course of preparation of [Zr-UiO-66-PDC-SO$_3$H]Cl. In continued, twice steps of weight losing (includes about 30% weight loss) was occurred about 300 °C which is linked to breaking the band of N-S of the structure of catalyst. Therefore, according to literature survey[13], the structure of [Zr-UiO-66-PDC-SO$_3$H]Cl is stable, even after adding sulfonic acidic functional groups.

For analyses the feature of the prepared functionalized MOFs, Surface area, pore volumes and pore size distribution were obtained using N_2 adsorption-desorption isotherm (Figure 6). The calculated of surface areas using BET equation , total pore volume and average pore size are 15.24 m^2 g^{-1}, 0.1914 cm^3 g^{-1} and 50.22 nm respectively.
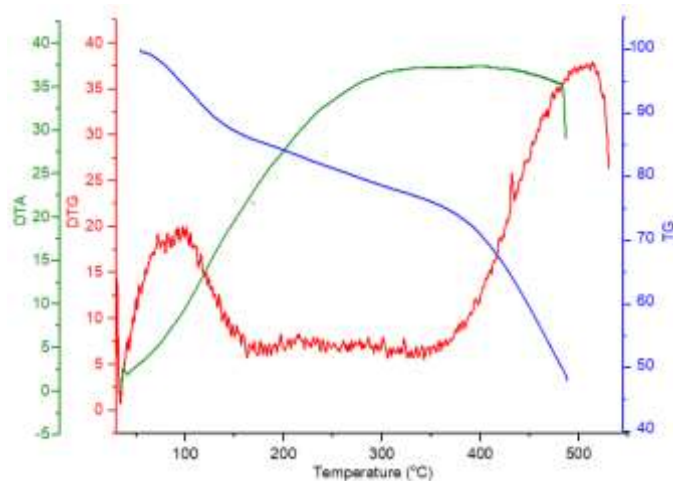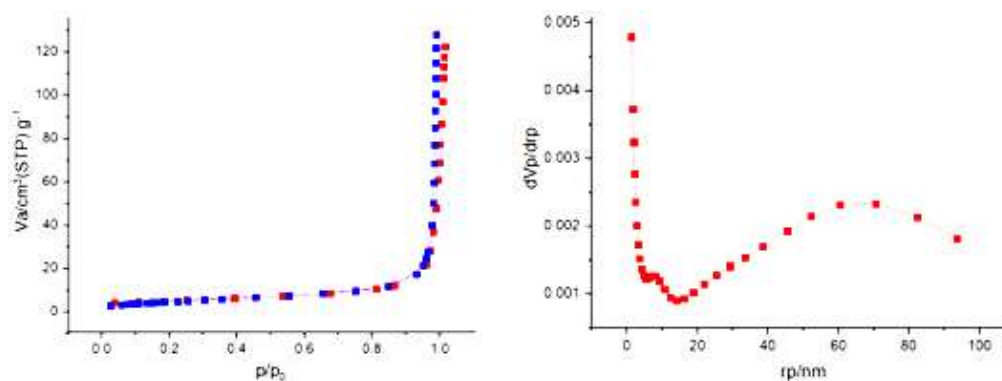
9

146

147

Figure 6. Up: TG, DTG and DTA analysis of [Zr-UiO-66-PDC-SO$_3$H]Cl. This figure was prepared by Microsoft Excel (OFFICE 2013). Down: N$_2$ adsorption/desorption isotherm and pore size distribution (BJH) of [Zr-UiO-66-PDC-SO$_3$H]Cl. This figure was prepared by Microsoft Excel (OFFICE 2013).

Also, we employed a cathodic (reductive) electrochemical technique for the preparation of Zr-UiO-66-PDC. As shown in Scheme 3, our procedure involves immersing a carbon electrode in a solution containing pyridine-2,5-dicarboxylic acid (H$_2$PDC) as a ligand, zirconium tetrachloride as a cation source and potassium nitrate as a supporting electrolyte. In-situ electrogeneration of hydroxide ions generated by electroreduction of water (as a co-solvent), NO$_3^-$ (as a counter ion) and/or direct deprotonation of ligand at 30.0 mA cm^{2-} for 1800 s is an essential requirement in this method. Increase in the local pH at the cathode surface causes activation of the ligands (deprotonation), and consequently formation of Zr-UiO-66-PDC through the coordination of activated ligands with zirconium cations (Figure 7).

10
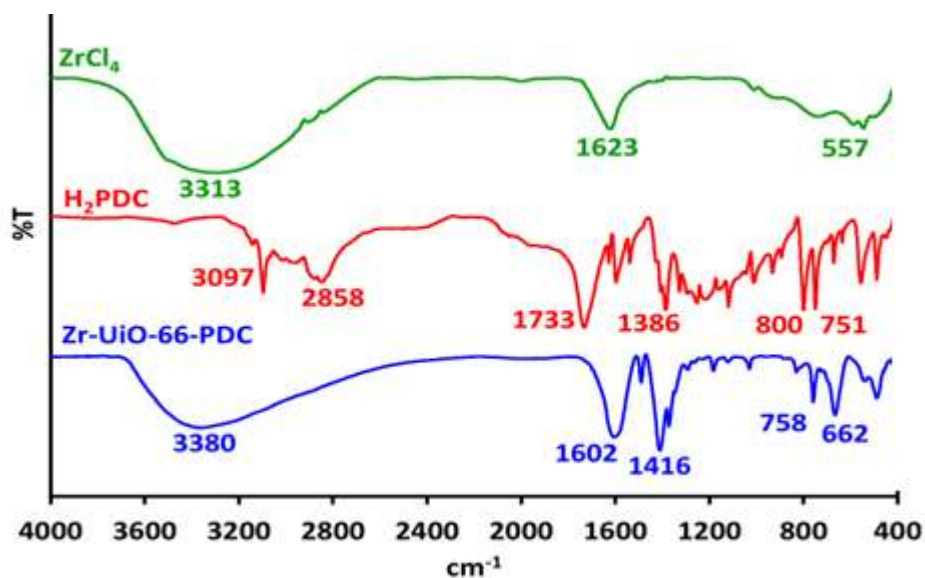
159

160

161 **Figure 7.** Up: Electrochemical synthesis of (UiO-66-PDC) by constant current electrolysis at I = 30 mA cm^{-2} and t =

162 1800 s. Down: Comparison of FT-IR spectra of pyridine-2,5-dicarboxylic acid (H$_2$PDC), ZrCl$_4$ and Zr-UiO-66-

163 PDC. The structures of the compounds were drawn using ChemOffice 12.0 (CambridgeSoft).

164   The nucleation rate and growth of Zr-UiO-66-PDC are only controlled by the cathodic reaction without the need

165 for any ex-situ base/probes additive, at room temperature, atmospheric pressure, and short time. Characterization of

166 the prepared Zr-UiO-66-PDC was examined by the FT-IR, FE-SEM and BET analysis. To confirm the functionality

11

167　and bonding groups of the electro-synthesized UiO-66-PDC MOF, FT-IR analysis was performed. The obtained

168　pattern is consistent with the reported pattern of chemical procedure (Figure 7).

169　　　Also, FE-SEM images of electro-synthesized (UiO-66-PDC) under constant current conditions shows the uniform

170　cauliflower-shape nanoparticles with an average diameter size of around 25.0 nm (Figure 8). This result is consistent

171　with the Zr based MOFs which prepared via pervious reported electrochemical synthesis [13].

172　　　This result is consistent with the Zr based MOFs which prepared via pervious reported electrochemical synthesis

173　[13]. The N_2 adsorption/desorption isotherm of Zr-UiO-66-PDC is shows in Figure 8 a "type IV" isotherm with a

174　hysteresis loop (between $p/p_0 = 0.4$ and 1) which is characteristic of mesoporous materials. Furthermore, the pore size

175　distribution obtained by the Barrett-Joyner-Halenda (BJH) method shows two peaks of 1.2 and 18.9 nm but the

176　average pore size is 13.4 nm. Besides, specific surface area measured from the N_2 isotherms is 181.64 m^2 g^{-1} that is

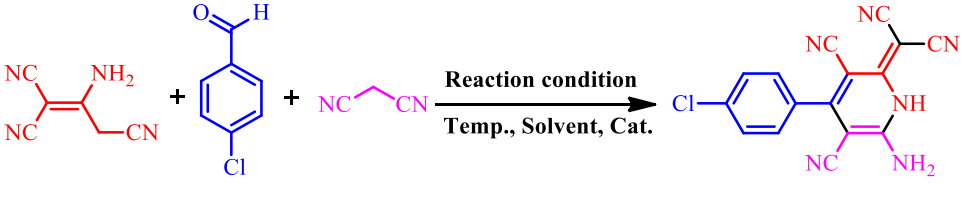177　higher than obtained amount of above mentioned hydrothermal and microwave methods.
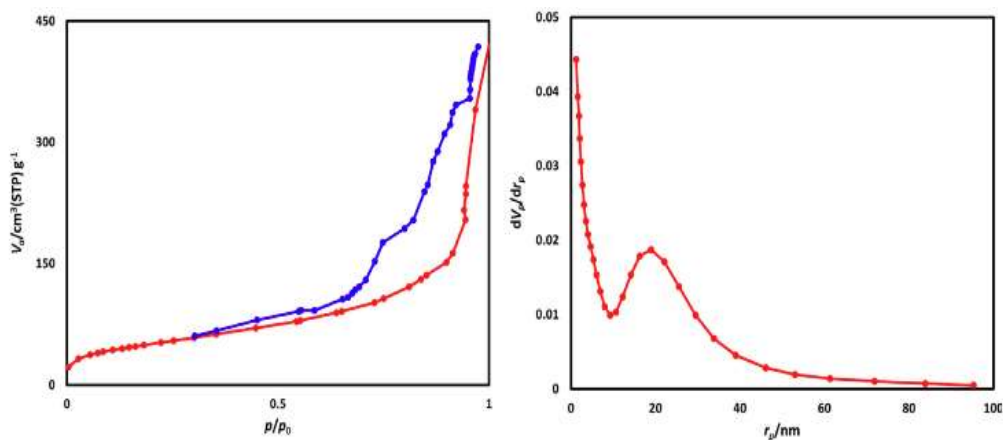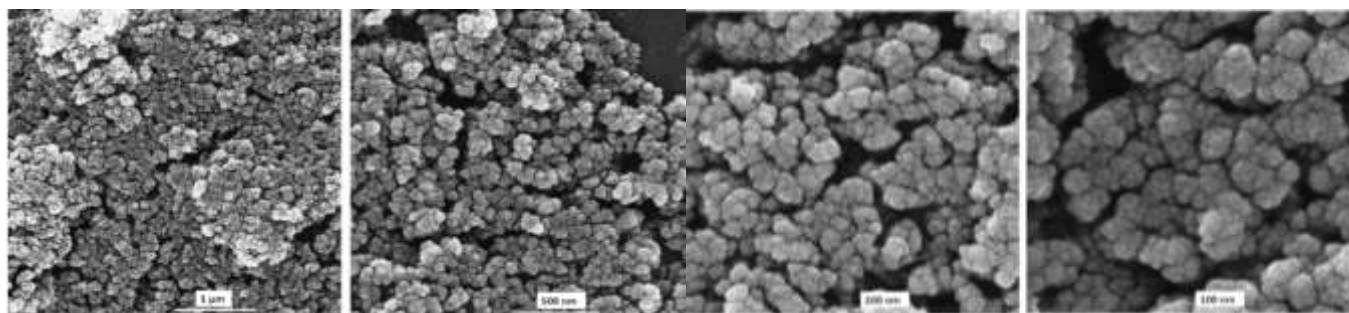
178

179

12

Figure 8. Up: Large- and close-view FE-SEM images of Zr-UiO-66-PDC by constant current electrolysis at I= 30 mA

cm^{-2} and t = 1800 s. Down: N_2 adsorption/desorption isotherm. BET and BJH of Zr-UiO-66-PDC by the constant

current electrolysis at I= 30 mA cm^{-2} and t = 1800 s.

Chemical and electrochemical synthesis of dicyanomethylene pyridine derivatives. Lately, a wide range of

dicyanomethylene pyridines was prepared via one-pot multicomponent condensation reactions in the presence of

a catalytic amounts of described [Zr-UiO-66-PDC-SO$_3$H]Cl as a mesoporous catalyst. The condensation of 4-chloro

benzaldehyde, 2-aminoprop-1-ene-1,1,3-tricarbonitrile and malononitrile was selected as a model for optimization

of the reaction conditions. As shown, the best condition reaction for the synthesis of 3,5-diaminobiphenyl-2,4,6-

tricarbonitrile was achieved in the presence of 10 mg [Zr-UiO-66-PDC-SO$_3$H]Cl in refluxing water (Table 1 entry 10).

Different amount of catalyst, temperature and solvent were not improved in the yield and time (Table 1 entries 1-

17 except 10). The obtained results of optimization reaction condition are summarized in Table 1.

Entry	Solvent (5 mL)	Cat. (mg)	Temp. (˚C)	Time (min)	Yield (%)
1	DMF	10	100	120	38
2	EtOH	10	Reflux	120	60
3	CH_2Cl_2	10	Reflux	120	63
4	$CHCl_3$	10	Reflux	120	20
5	EtOAc	10	Reflux	120	40
6	CH_3CN	10	Reflux	120	58
7	PEG	10	Reflux	120	35
8	n-Hexane	10	Reflux	120	65
9	H_2O	10	Reflux	120	52

13

10	-	10	100	20	87
11	-	5	100	30	75
12	-	15	100	30	87
13	-	20	100	30	85
14	-	10	25	120	15
15	-	10	50	120	68
16	-	-	75	120	10
17	-	10	100	120	70

Table 1. Effect of different amounts of catalyst, temperature and solvent (5 mL) in the synthesis dicyanomethylene pyridine.

After optimization reaction condition, the scope and limitations of [Zr-UiO-66-PDC-SO3H]Cl as as a novel catalyst was investigated in the preparation of dicyanomethylene pyridine via a condensation reaction of widespread analog of aldehyde (mono, bis and tris substituted C=O) which are bearing electron-donating and electron-withdrawing groups, malononitrile and 2-aminoprop-1-ene-1,1,3-tricarbonitrile. As shown in Table 2, the results indicated that this strategy is appropriate for the synthesis of dicyanomethylene pyridine (Table 2).
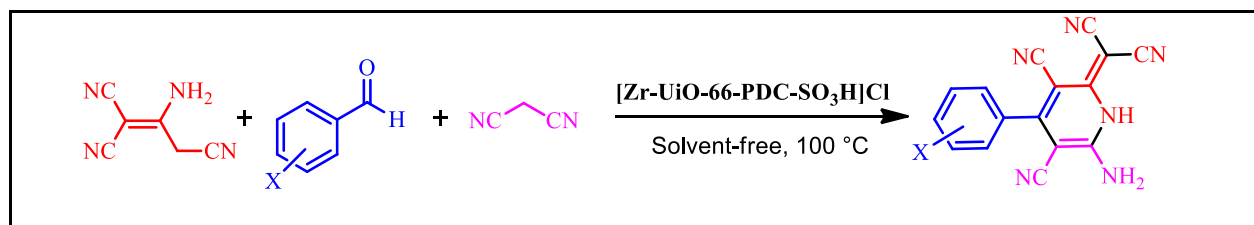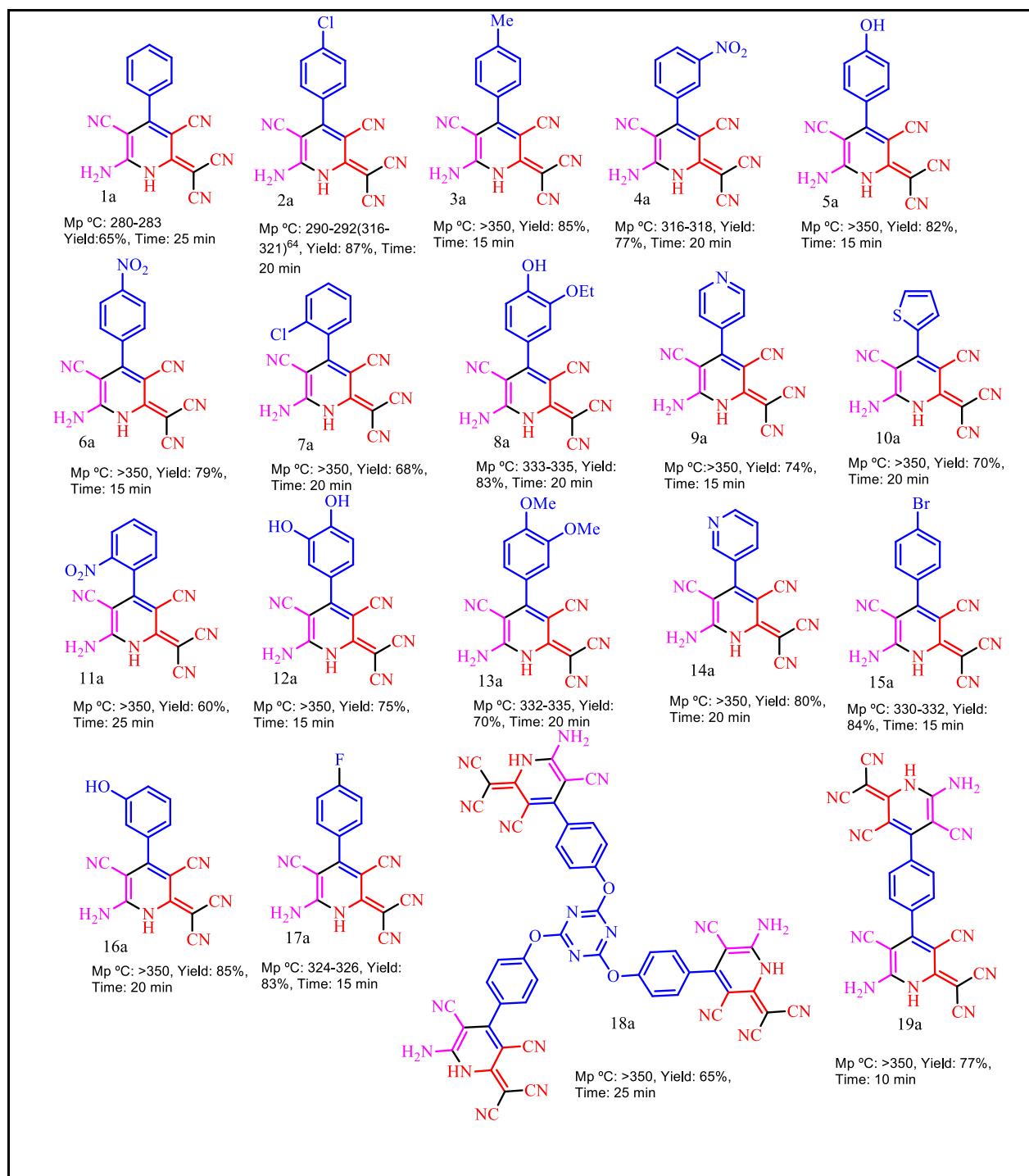
Table 2: Effect of different amounts of catalyst, temperature and solvent (5 mL) in the synthesis dicyanomethylene pyridine.

Proposed mechanism for the synthesis of dicyanomethylene pyridine derivatives using [Zr-UiO-66-PDC-SO₃H]Cl was summarized in Scheme 6. The SO₃H group of [Zr-UiO-66-PDC-SO₃H]Cl is activing the carbonyl group of aldehyde. In the first step, malononitrile is reacting with the carbonyl group of aldehyde to afford Knoevenagel's

15

203 adduct **I** by removing one molecule of H_2O. Then, 2-aminoprop-1-ene-1,1,3-tricarbonitrile attacks to **I** to give

204 intermediate **II**, which is reacting to give **III** *via* an intramolecular cyclocondensation. Finally, the intermediate **III**

205 and **IV** was converted to the desired product **VI** through intermediate **V** *via* a cooperative vinylogous ABO and

206 releasing one molecule of hydrogen (H_2) (Figure 9).[33]

207 The obtained results from model reaction under argon and nitrogen atmospheres verified abovementioned our

208 suggestion for latter step. Literature survey shows that there is no a rational and clear stepwise mechanism for

209 synthesis of the presented molecules [64,65]. Herein, we wish to present a comprehensive mechanism for mentioned

210 reaction so that its final step might be progress through a cooperative vinylogous ABO in the absence of oxygen

211 molecules. In the intermediates **III** and **IV,** sharing the electron density from the endo and exo nitrogens lone pairs

212 to the vacant antibonding σ^* orbital of SP^3 C-H bond through vinylic C=C double bonds support the unusual hydride

213 transfer for releasing the molecular hydrogen (H_2). Recently, we have been named this phenomenon as a new term

214 entitled a cooperative vinylogous ABO and its development for various catalytic systems is our main research interest

215 [30-38]. The described ABO mechanism is in good agreement with the "vinylogous anomeric effect" concept which at

216 first, had been introduced by Katritzky [66].

217 At the second step of this work, [Zr-UiO-66-PDC-SO$_3$H]Cl was employed for the preparation of dihydropyridine

218 compounds via convergent paired electrosynthesis as green and sustainable technique. To shed light on this fact, as

219 shown in Figure 10, an undivided home-made cell comprising two electrodes under constant current electrolysis was

220 employed for this purpose. The convergent paired electrosynthesis was started by applying constant current

221 electrolysis (CCE) (1 mA cm^{-2}) in ethanol and room temperature as green conditions. Upon the starting electrolysis,

222 malononitrile can be activated to the methylene malononitrile on the cathodic electrode without need to the ex-situ

223 base additive. At the other hands, activation of carbonyl group of aldehyde can be done by the SO_3H functional group

224 of employed catalysis, simultaneously. So, the suitable condition for preparing of the knoevenagel's adduct (**I**) will

225 be provided through attacking of the methylene malononitrile on the activated aldehyde and removing of one H_2O

226 molecule. At the second step, 2-aminoprop-1-ene-1,1,3-tricarbonitrile can be attacked to the in-situ prepared

227 knoevenagel's adduct (**I**) via the Michel addition reaction.
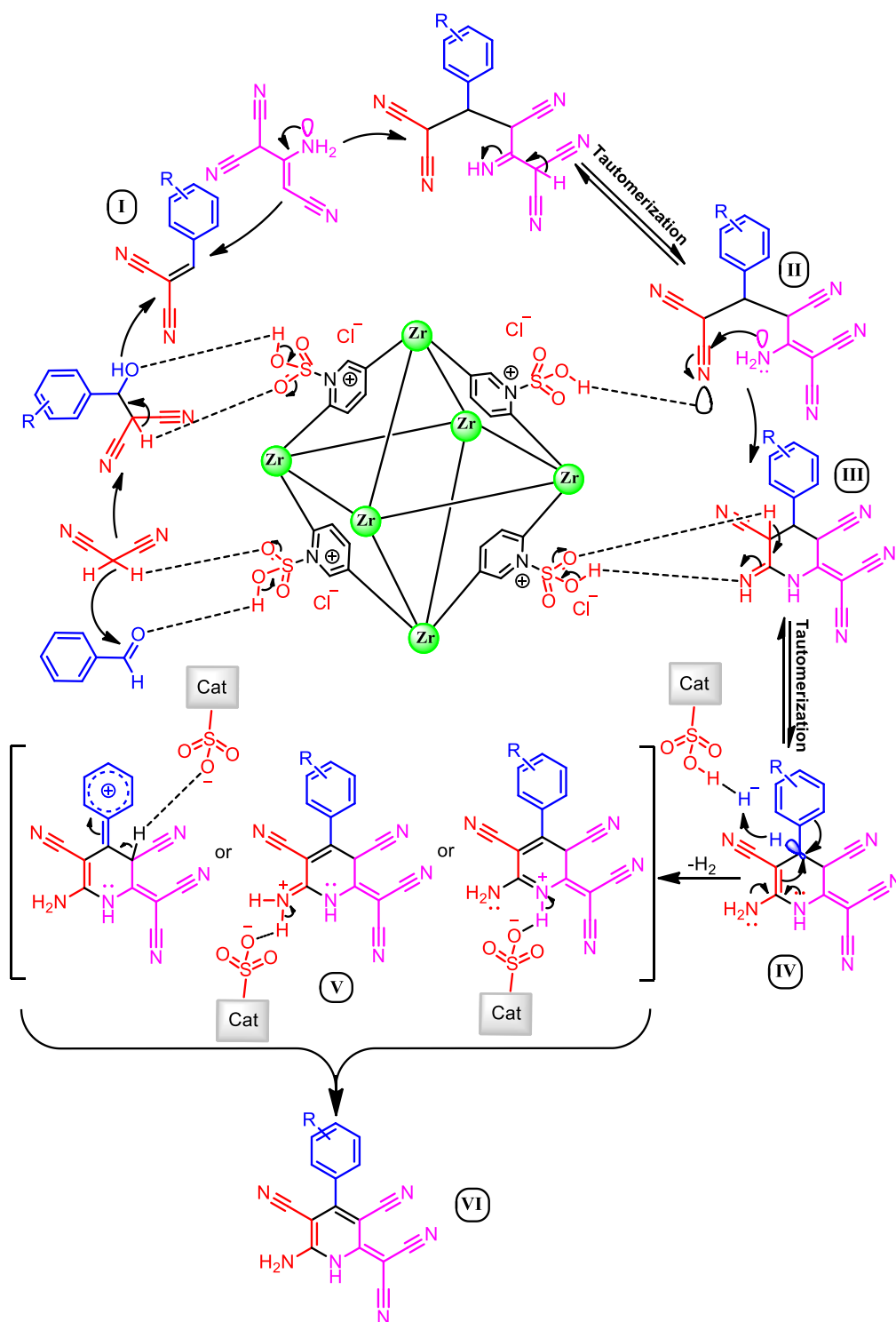
16

228

Figure 9. A rational proposed mechanism for the synthesis of dicyanomethylene pyridine using [Zr-UiO-66-PDC-SO₃H]Cl.

231
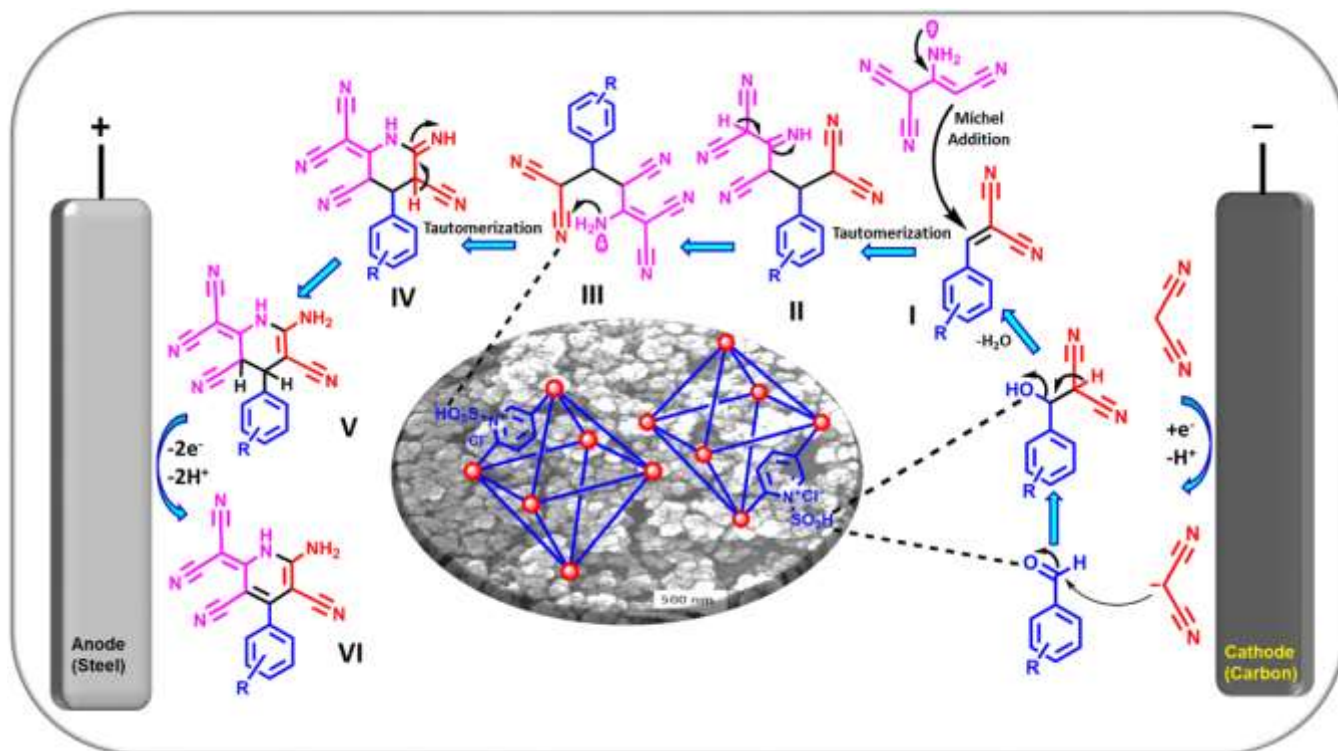
Figure 10. Convergent paired electrochemical synthesis of dicyanomethylene pyridine compounds.

After tautomerization step (**II**), the produced intermediate (**III**) undergoes an intramolecular cyclocondensation by effective activation of nitrile functional group via SO_3H functional group of employed catalysis.

Finally, in order to the implementation and completing of the convergent paired electrosynthesis the produced intermediate (**V**) after tautomerization step (**IV**), can be oxidized on the anodic electrode by releasing of two electron/two proton, in order to harvesting the final product (**VI**). It should be noted, the progress and yield of reaction in the absence of the [Zr-UiO-66-PDC-SO_3H]Cl catalyst was slow and low.

It is noteworthy mention that, the higher applied currents lead to the occurrence of side reactions like polymerization of malononitrile and the lower applied currents lead to prolonged reaction time or low yields due to the inactivation of malononitrile. Table 3 indicate the optimization of applied current density at the electrolysis condition.
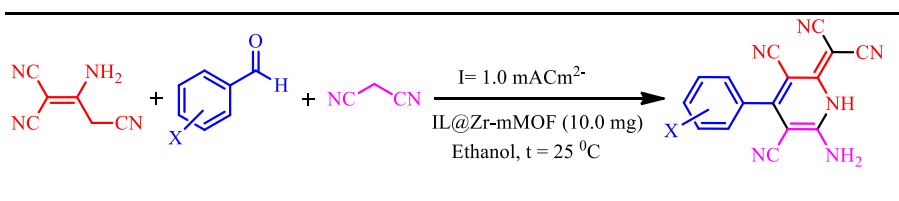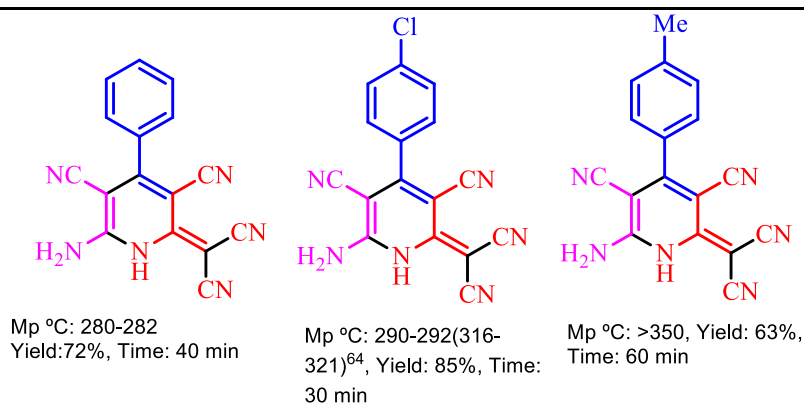
18

Table 3. Optimization of conditions for the synthesis of dicyanomethylene pyridine.
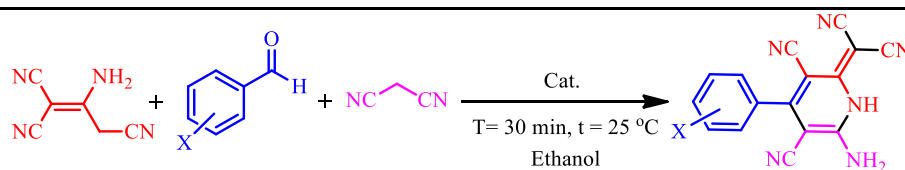
Substrate	Current Density (mA cm$^{2\text{-}}$)	Yield (%)
4-Chlorobenzaldehyde	0.5	35
4-Chlorobenzaldehyde	1.0	85
4-Chlorobenzaldehyde	1.5	25

Table 4 indicates the results of the model reactions based on the electronic properties of substitute groups on the benzaldehyde. The data presented in Table 4 shows the applied procedure have a satisfying performance for electrosynthesis of related dihydropyridine derivatives in a one-pot reaction with a 63–85 % overall yield. It is noteworthy to mention that, the higher product yield for aldehydes with electron-withdrawing groups, 4-Chlorobenzaldehyde, is comparable and even greater than that of their simple (benzaldehyde) and/or electron-donating (4-methylbenzaldehyde) group homologues. This results may be caused by more efficient deprotonation of related aldehydes bearing electron-withdrawing groups lead to an intermediate under the proposed mechanism. So, the obtained trend may be repeated for the other homologue aldehydes based on the electron characteristics of substituted groups with acceptable tolerance.

19

Mp ºC: 280-282
Yield:72%, Time: 40 min

Mp ºC: 290-292(316-321)[64], Yield: 85%, Time: 30 min

Mp ºC: >350, Yield: 63%, Time: 60 min

Table 4. Electrochemical synthesis of dicyanomethylene pyridine derivatives in the presence of [Zr-UiO-66-PDC-SO$_3$H]Cl as a catalyst. At the I= 1.0 mA cm^{-2}.

To evaluate the performance of [Zr-UiO-66-PDC-SO$_3$H]Cl as an efficient catalyst for the synthesis of dicyanomethylene pyridine, we have tested different acid catalysts (organic and inorganic) by reaction of 4-chloro benzaldehyde (1 mmol, 0.14 g), 2-aminoprop-1-ene-1,1,3-tricarbonitrile (1 mmol, 0.132 g), and malononitrile (1.1 mmol, 0.072 g) in Table 5. As a results in Table 5, [Zr-UiO-66-PDC-SO$_3$H]Cl is the best catalyst for the synthesis of dicyanomethylene pyridine.
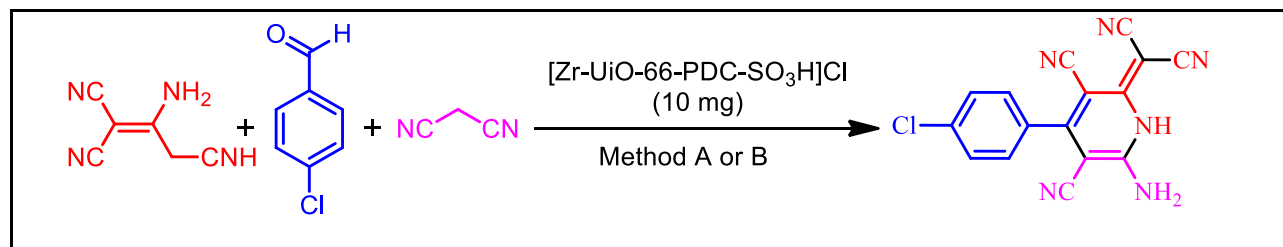
Entry	Catalyst	(mol%)	Time (min)	Yield (%)
1	SSA	10	120	Trace
2	H$_2$SO$_4$	10	120	20
3	Fe$_3$O$_4$	10 mg	120	18
4	*p*-TSA	10	120	-
5	[PVI-SO$_3$H]Cl	10 mg	120	43
6	MIL-100(Cr)/NHEtN(CH$_2$PO$_3$H$_2$)$_2$	10 mg	120	56
7	Trichloroisocyanuric acid	10	120	-
8	Al(HSO$_4$)$_3$	10	120	-

20

9	Mg(NO$_3$)$_2$.6H$_2$O	10	120	28
10	NaHSO$_4$	10	120	-
11	NH$_4$NO$_3$	10	120	-
12	FeCl$_3$	10	120	38
13	H$_3$[p(Mo$_3$O$_{10}$)$_4$].XH$_2$O	10	120	-
14	Zn(NO$_3$)$_2$.6H$_2$O	10	120	25
15	KOH	10	120	Trace

260   **Table 5**: Evaluation of various catalysts for the synthesis of dicyanomethylene pyridine in comparison with [Zr-UiO-

261   66-PDC-SO$_3$H]Cl.

262   Results of catalytic activity and reusability of [Zr-UiO-66-PDC-SO$_3$H]Cl were added in Figure 11. [Zr-UiO-66-

263   PDC-SO$_3$H]Cl can be separated by centrifugation and reused without significantly reducing its catalytic reactivity.

264   For this purpose, recyclability of the catalyst was studied on the reaction of 4-chloro benzaldehyde (1 mmol, 0.14 g),

265   2-aminoprop-1-ene-1,1,3-tricarbonitrile (1 mmol, 0.132 g), and malononitrile (1.1 mmol, 0.072 g) as a model reaction

266   under the above mentioned optimized reaction conditions. Therefore, [Zr-UiO-66-PDC-SO$_3$H]Cl can be reused up to

267   six times without noticeable changes in its catalytic activity.
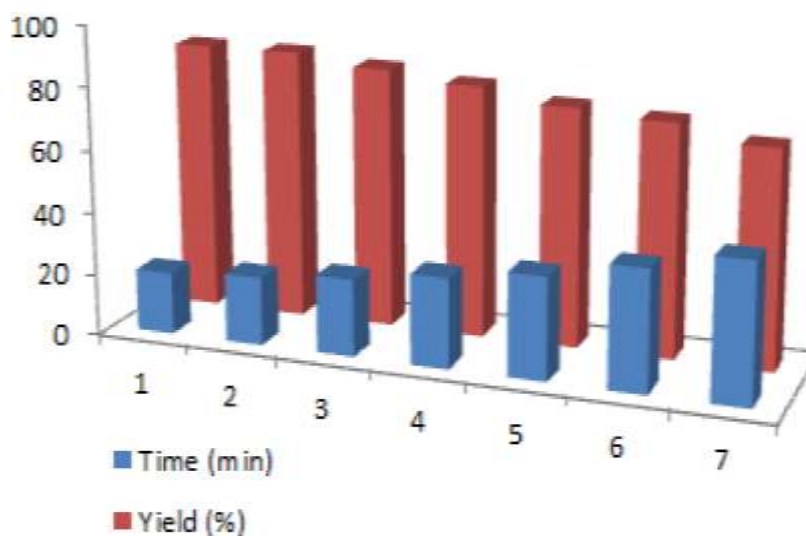
268

269   **Figure 11**: Recyclability of of [Zr-UiO-66-PDC-SO$_3$H]Cl at the synthesis (2-methyl-1*H*-indol-3-yl)-pyrazolo[3,4-

270   *b*]pyridine derivatives.

21

Conclusions

In this study, we have introduced a novel Zr-metal-organic frameworks [Zr-UiO-66-PDC-SO$_3$H]Cl as a mesoporous catalyst. This catalyst was tested for the preparation of various novel dicyanomethylene pyridine via a cooperative vinylogous anomeric based oxidation mechanism. Topology of the [Zr-UiO-66-PDC-SO$_3$H]Cl was also characterized by SEM and TEM images. As well as, thermal and solvent stability of the catalyst are high after reaction of SO$_3$HCl with [Zr-UiO-66-PDC]. Furthermore, the major advantages of the presented work are mild and green conditions, high yields, short reaction times, facile workup and reusability of the described [Zr-UiO-66-PDC-SO$_3$H]Cl. Also, this paper provides a green and promising electrochemical procedure for the preparation of mesoporous (UiO-66-PDC). From the standpoint of environmental issues, synthesis of these compounds can be performed without the need for any ex-situ chemical agent such as a base or probase. On the other hands, the use of electricity eliminates the need for high temperature and pressure, which is the most outstanding features of this study. Furthermore, the convergent paired electrosynthesis of dicyanomethylene pyridine derivatives with the prepared catalyst was performed as an environmental friendly technique under green conditions, at room temperature and pressure. We think that, the present work is a promising insight for inter and multidisciplinary research, rational design, syntheses and applications of task-specific MOFs and bioactive molecules.

Materials and Methods

Pyridine-2,5-dicarboxylic acid (H$_2$PDC) (Merck, 95%), Zirconium tetrachloride (ZrCl$_4$) (Sigma Aldrich, 98%), Potassium Nitrate (KNO$_3$) (Sigma-Aldrich, 99%), formic acid (HCOOH) (Merck, 37%), Ethanol (C$_2$H$_5$OH) (Merck, 99%), Lithium Perchlorate (LiClO$_4$) (Merck, 99%) and other materials (Merck) were reagent-grade materials and used as received without further purification. All solutions were prepared at the room temperature. The known products were identified by comparison of their melting points and spectral data with those reported in the literature. To scrutinize the progress of the reaction, silica gel SIL G/UV 254 plates were used. From the model of the BRUKER Ultrashield FT-NMR spectrometer (δ in ppm) were recorded ^{1}H NMR (600 or 400 MHz)

22

and ^{13}C NMR (151 or 101 MHz). Recorded on a Büchi B-545 apparatus in open capillary tubes were melting points. The PerkinElmer PE-1600-FTIR device was recorded for infrared spectra of compounds. SEM was performed using a scanning electron microscope for field publishing made by TE-SCAN. Thermal gravimetry (TG), differential thermal gravimetric (DTG) and differential thermal (DTA) were analyzed by a Perkin Elmer (Model: Pyris 1). BET and BJH were analyzed by BELSORP-mini ii high precision Surface area and pore size.

Electrosynthesis Setup

Electrosynthesis of catalyst and dicyanomethylene pyridine compounds were performed in a homemade undivided two-electrode cell. The cell consists of a cap glass bottle containing a precursor solution, carbon plate as working electrode (100 mm × 20 mm × 5 mm) and the U-shape stainless steel sheet as the auxiliary electrode. All of the electrochemical synthesis experiments were done at room temperature and pressure. Electrosynthesis of [Zr-UiO-66-PDC-SO$_3$H]Cl and dicyanomethylene pyridine derivatives were accomplished by applying a suitable current density for a specified period.

Chemical procedure for the preparation of Zr-UiO-66-PDC

In a 100 mL round-bottomed flask, a mixture of pyridine-2,5-dicarboxylic acid (H$_2$PDC) (0.366 g, 2.2 mmol) and ZrCl$_4$ (0.512 g, 2.2 mmol) with formic acid and H$_2$O (9:1) 50 mL as solvent were stirred at 120 °C for 3 h under reflux conditions. [13] After this time, the suspension was filtered by centrifugation (2000 rpm, 20 min). Then, to the sediment was added H$_2$O which was separated by centrifugation (2000 rpm, 20 min, 3 run). Finally, white precipitate was dried under a powerful vacuum at 90 °C to give Zr-UiO-66-PDC (Figure 12).
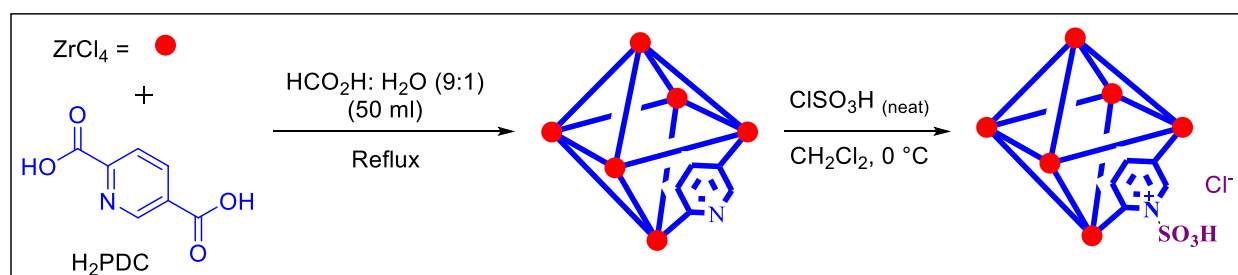
Figure 12. Chemical synthesis of [Zr-UiO-66-PDC-SO$_3$H]Cl as a functionalized MOF catalyst

23

General procedure for the preparation of [Zr-UiO-66-PDC-SO3H]Cl

In a 50 mL round-bottomed flask, a mixture of Zr-UiO-66-PDC (1 mmol, 0.282 g) and chlorosulfonic acid (1 mmol, 0.067 mL) in dry CH_2Cl_2 (20 mL) at 0 °C were stirred for 2 hours. Then, the sediment appeared which was filtered by centrifugation (1000 rpm, 5 min, 2 time) and dried under vacuum to obtain white precipitated as [Zr-UiO-66-PDC-SO_3H]Cl (Figure 12).

Chemical procedure for the preparation of dicyanomethylene pyridine derivatives using [Zr-UiO-66-PDC-SO_3H]Cl as an efficient catalyst

In a 15 mL round-bottomed flask, a mixture of aldehyde (1 mmol, 0.398 g), 2-aminoprop-1-ene-1,1,3-tricarbonitrile (1 mmol, 0.132 g) and malononitrile (1.1 mmol, 0.073 g) and [Zr-UiO-66-PDC-SO_3H]Cl (10 mg) as catalyst was stirred under solvent-free conditions at 100 ∘C. After completion of the reaction which was followed by TLC (*n*-hexane: ethyl acetate; 7:3), the reaction mixture was cool down to room temperature. Then, the mixture was added 10 mL ethanol and the catalyst was subsequently removed by centrifugation (1000 rpm). Finally, the product was recrystallized with EtOH (Figure 2).

Electrochemical procedure for the preparation of Zr-UiO-66-PDC

In typical procedure, (0.512 g, 2.2 mmol) of zirconium tetrachloride as a cation source, (0.366 g, 2.2 mmol) of pyridine-2,5-dicarboxylic acid (H_2PDC) as ligand and (0.127 g, 0.1 mmol) potassium nitrate (KNO_3) as a supporting electrolyte were dissolved in the 50.0 mL aqueous solution of formic acid (H_2O/formic acid; 1/9). The solution was stirred at room temperature for 30 min before the electrolysis (30 mAcm^{2-} for 1800 s). After electrolysis, the solution was centrifuged at 5000 rpm for 5 min, and the precipitate was washed twice with distilled water and ethanol. The final MOF was then aged overnight at the 100 °C.

Electrochemical procedure for convergent paired electrosynthesis of dicyanomethylene pyridines

24

The convergent paired electrosynthesis of dicyanomethylene pyridines derivatives was carried out in 50 mL of ethanol containing aldehyde derivatives (1.0 mmol), malononitrile (0.066 g, 1.0 mmol), 2-aminoprop-1-ene-1,1,3-tricarbonitrile (0.132 g, 1.0 mmol) and [Zr-UiO-66-PDC-SO$_3$H]Cl (10.0 mg) as catalyst under stirring at 1.0 mA cm^{-2}. The progress of the reaction was detected by thin-layer chromatography (*n*-hexane; ethylacetate). The final product was separated by thin-layer chromatography.

Characteristic of the products

6-Amino-2-(dicyanomethylene)-4-phenyl-1,2-dihydropyridine-3,5-dicarbonitrile (1a). Yellow solid; Mp: 280-283 °C; IR (KBr): υ (cm^{-1}) = 3374, 3306, 3215, 2218, 2191, 1642. ^{1}H NMR (400 MHz, DMSO-d_6) δ 7.80 (s, 3H), 7.60 − 7.53 (m, 3H), 7.48 (d, *J* = 1.3 Hz, 2H). ^{13}C NMR (101 MHz, DMSO-d_6) δ 160.5, 160.4, 157.8, 135.3, 129.7, 128.4, 128.3, 116.2, 115.9, 85.4, 80.7, 43.6.

6-Amino-4-(4-chlorophenyl)-2-(dicyanomethylene)-1,2-dihydropyridine-3,5-dicarbonitrile (2a). Yellow solid; Mp: 290-262 °C; IR (KBr): υ (cm^{-1}) = 3363, 3302, 3211, 2228, 2217, 2191, 1645. ^{1}H NMR (600 MHz, DMSO-d_6) δ 7.59 (d, J = 8.4 Hz, 2H), 7.46 (d, J = 8.4 Hz, 2H), 6.52 (s, 3H). ^{13}C NMR (151 MHz, DMSO-d_6) δ 161.6, 159.5, 158.5, 134.9, 134.9, 130.8, 129.1, 116.8, 116.5, 85.6, 81.0, 44.2.

6-Amino-2-(dicyanomethylene)-4-(p-tolyl)-1,2-dihydropyridine-3,5-dicarbonitrile (3a). Yellow solid; Mp: >350 °C; IR (KBr): υ (cm^{-1}) = 3483, 3371, 3202, 2213, 2200, 2171, 1620. ^{1}H NMR (400 MHz, DMSO-d_6) δ 7.29 (s, 4H), 6.87 (s, 2H), 2.38 (s, 3H). ^{13}C NMR (101 MHz, DMSO-d_6) δ 162.7, 159.7, 158.7, 139.0, 132.8, 128.9, 128.3, 116.9, 116.6, 85.0, 80.3, 20.9.

6-Amino-2-(dicyanomethylene)-4-(3-nitrophenyl)-1,2-dihydropyridine-3,5-dicarbonitrile (4a). Yellow solid; Mp: 316-318 °C; IR (KBr): υ (cm^{-1}) = 3438, 3339, 3213, 2197, 2181, 1657, 1556, 1352. ^{1}H NMR (600 MHz, DMSO-d_6) δ 8.38 − 8.35 (m, 1H), 8.33 − 8.30 (m, 1H), 7.93 (d, *J* = 7.7 Hz, 1H), 7.83 (t, *J* = 8.0 Hz, 1H), 7.05 (s, 2H). ^{13}C NMR (151 MHz, DMSO-d_6) δ 163.0, 159.0, 157.9, 148.0, 137.8, 135.9, 130.8, 124.8, 123.9, 117.1, 116.9, 85.3, 80.7, 44.3.

357 *6-Amino-2-(dicyanomethylene)-4-(4-hydroxyphenyl)-1,2-dihydropyridine-3,5-dicarbonitrile (5a).* Yellow solid; Mp:

358 >350 °C; IR (KBr): υ (cm^{-1}) = 3342, 3227, 2183, 1652, 1553. ^{1}H NMR (600 MHz, DMSO-d_6) δ 9.85 (s, 1H), 7.23 (d, *J* =

359 8.5 Hz, 2H), 6.89 – 6.78 (m, 4H). ^{13}C NMR (151 MHz, DMSO-d_6) δ 163.4, 160.1, 159.3, 159.1, 130.6, 126.6, 117.7,

360 117.3, 115.5, 85.6, 80.7, 43.6.

361 *6-Amino-2-(dicyanomethylene)-4-(4-nitrophenyl)-1,2-dihydropyridine-3,5-dicarbonitrile (6a).* Yellow solid; Mp:

362 >350 °C; IR (KBr): υ (cm^{-1}) = 3336, 2196, 1655, 1556, 1508, 1360. ^{1}H NMR (600 MHz, DMSO-d_6) δ 8.35 (d, *J* = 8.7

363 Hz, 2H), 7.74 (d, *J* = 8.7 Hz, 2H), 7.05 (s, 2H). ^{13}C NMR (151 MHz, DMSO-d_6) δ 162.9, 159.0, 158.3, 148.5, 142.9,

364 130.7, 124.1, 116.9, 116.7, 85.0, 80.4, 44.3.

365 *6-Amino-4-(2-chlorophenyl)-2-(dicyanomethylene)-1,2-dihydropyridine-3,5-dicarbonitrile (7a).* Yellow solid; Mp:

366 >350 °C; IR (KBr): υ (cm^{-1}) = 3438, 3342, 3231, 2195, 2164, 1636, 1557. ^{1}H NMR (600 MHz, DMSO-d_6) δ 7.61 (dd, *J*

367 = 7.9, 1.3 Hz, 1H), 7.50 (td, *J* = 7.7, 1.9 Hz, 1H), 7.47 (td, *J* = 7.5, 1.4 Hz, 1H), 7.40 (dd, *J* = 7.4, 1.8 Hz, 1H), 7.00 (s,

368 2H). ^{13}C NMR (151 MHz, DMSO-d_6) δ 162.7, 158.9, 157.9, 135.5, 131.6, 131.4, 130.7, 130.0, 128.0, 116.6, 116.3,

369 86.0, 81.1, 44.0.

370 *6-Amino-2-(dicyanomethylene)-4-(3-ethoxy-4-hydroxyphenyl)-1,2-dihydropyridine-3,5-dicarbonitrile (8a).* Yellow

371 solid; Mp: 333-335 °C; IR (KBr): υ (cm^{-1}) = 3431, 3342, 3236, 2198, 2165, 1649, 1554. ^{1}H NMR (600 MHz, DMSO-d_6)

372 δ 9.38 (s, 1H), 6.97 – 6.94 (m, 1H), 6.87 (d, *J* = 8.1 Hz, 1H), 6.85 – 6.78 (m, 3H), 4.06 (q, *J* = 7.0 Hz, 2H), 1.36 – 1.33

373 (m, 3H). ^{13}C NMR (151 MHz, DMSO-d_6) δ 163.3, 160.1, 159.3, 148.6, 146.5, 126.8, 122.1, 117.8, 117.4, 115.7, 114.6,

374 85.6, 80.8, 64.3, 43.6, 15.1.

375 *6-Amino-2-(dicyanomethylene)-1,2-dihydro-[4,4'-bipyridine]-3,5-dicarbonitrile (9a).* Yellow solid; Mp: >350 °C; IR

376 (KBr): υ (cm^{-1}) = 3443, 3345, 3224, 2211, 2195, 2175, 1650, 1569. ^{1}H NMR (600 MHz, DMSO-d_6) δ 8.72 (d, *J* = 5.7

377 Hz, 2H), 7.46 (d, *J* = 4.4 Hz, 2H), 7.04 (s, 2H). ^{13}C NMR (151 MHz, DMSO-d_6) δ 162.9, 159.0, 157.7, 150.3, 144.2,

378 123.6, 116.9, 116.6, 84.7, 80.1, 44.3.

26

379 *6-Amino-2-(dicyanomethylene)-4-(thiophen-2-yl)-1,2-dihydropyridine-3,5-dicarbonitrile (10a).* Yellow solid; Mp:

380 >350 °C; IR (KBr): υ (cm⁻¹) = 3481, 3345, 3211, 2213, 2189, 2163, 1624, 1555. ^{1}H NMR (600 MHz, DMSO-d_6) δ 7.82

381 (d, *J* = 4.9 Hz, 1H), 7.37 (d, *J* = 3.5 Hz, 1H), 7.23 − 7.18 (m, 1H), 6.97 (s, 2H). ^{13}C NMR (151 MHz, DMSO-d_6) δ 163.4,

382 159.3, 152.2, 135.2, 130.4, 129.6, 127.9, 117.3, 116.9, 85.8, 81.0, 44.2.

383 *6-Amino-2-(dicyanomethylene)-4-(2-nitrophenyl)-1,2-dihydropyridine-3,5-dicarbonitrile (11a).* Yellow solid; Mp:

384 >350 °C; IR (KBr): υ (cm⁻¹) = 3437, 3341, 3230, 2218, 2195, 1637, 1560, 1517, 1351. ^{1}H NMR (600 MHz, DMSO-d_6)

385 δ 8.27 (d, *J* = 8.2 Hz, 1H), 7.92 (t, *J* = 7.5 Hz, 1H), 7.80 (t, *J* = 7.9 Hz, 1H), 7.60 (d, *J* = 7.5 Hz, 1H), 7.05 (s, 2H). ^{13}C NMR

386 (151 MHz, DMSO-d_6) δ 170.8, 162.6, 158.8, 158.1, 147.3, 135.2, 131.8, 131.6, 131.3, 125.4, 116.6, 116.4, 84.9, 80.2,

387 60.2, 44.1, 21.2, 14.6.

388 *6-Amino-2-(dicyanomethylene)-4-(3,4-dihydroxyphenyl)-1,2-dihydropyridine-3,5-dicarbonitrile (12a).* Yellow solid;

389 Mp: >350 °C; IR (KBr): υ (cm⁻¹) = 3457, 3334, 3225, 2197, 2168, 1650, 1560. ^{1}H NMR (600 MHz, DMSO-d_6) δ 9.33

390 (s, 1H), 9.26 (s, 1H), 6.80 (d, *J* = 8.0 Hz, 3H), 6.77 (s, 1H), 6.67 (d, *J* = 8.1 Hz, 1H).

391 *6-Amino-2-(dicyanomethyl)-4-(3,4-dimethoxyphenyl)-1,2-dihydropyridine-3,5-dicarbonitrile (13a).* Yellow solid;

392 Mp: 332-335 °C; IR (KBr): υ (cm⁻¹) = 3504, 3489, 3374, 2216, 2194, 2172, 1613, 1551. ^{1}H NMR (400 MHz, DMSO-d_6)

393 δ 7.07 (d, *J* = 8.3 Hz, 1H), 7.03 (d, *J* = 2.1 Hz, 1H), 6.97 (dd, *J* = 8.2, 2.1 Hz, 1H), 6.88 (s, 2H), 3.82 (s, 3H), 3.79 (s, 3H).

394 ^{13}C NMR (101 MHz, DMSO-d_6) δ 162.7, 159.3, 158.8, 149.6, 148.0, 127.7, 121.3, 117.1, 116.7, 112.2, 111.2, 85.1,

395 80.3, 55.5, 55.4, 43.1, 40.0.

396 *6'-Amino-2'-(dicyanomethylene)-1',2'-dihydro-[3,4'-bipyridine]-3',5'-dicarbonitrile (14a).* Brown solid; Mp: >350 °C;

397 IR (KBr): υ (cm⁻¹) = 3389, 3317, 3161, 2209, 2189, 2156, 1654, 1577, 1514. ^{1}H NMR (400 MHz, DMSO-d_6) δ 8.79 −

398 8.47 (m, 2H), 7.91 (dt, *J* = 7.9, 2.0 Hz, 1H), 7.55 (dd, *J* = 7.9, 4.9 Hz, 1H), 7.03 (s, 2H). ^{13}C NMR (101 MHz, DMSO-d_6)

399 δ 162.52, 158.57, 156.38, 150.38, 148.47, 136.39, 131.89, 123.40, 116.65, 116.43, 85.08, 80.40, 40.03.

400 *6-Amino-4-(4-bromophenyl)-2-(dicyanomethylene)-1,2-dihydropyridine-3,5-dicarbonitrile (15a).* White solid; Mp:

401 330-332 °C; IR (KBr): υ (cm⁻¹) = 3451, 3339, 3224, 2214, 2194, 2170, 1674, 1572, 1511. ^{1}H NMR (400 MHz, DMSO-

27

d_6) δ 7.77 – 7.64 (m, 2H), 7.46 – 7.30 (m, 2H), 6.97 (s, 2H). ^{13}C NMR (101 MHz, DMSO-d_6) δ 162.5, 158.5, 158.5, 135.0, 131.4, 130.6, 123.0, 116.7, 116.4, 84.8, 80.1, 40.0.

6-Amino-2-(dicyanomethylene)-4-(3-hydroxyphenyl)-1,2-dihydropyridine-3,5-dicarbonitrile (16a). Yellow solid; Mp: >350 °C; IR (KBr): υ (cm^{-1}) = 3476, 3330, 3218, 2202, 2171, 1625, 1548. ^{1}H NMR (600 MHz, DMSO-d_6) δ 9.72 (s, 1H), 7.28 (t, *J* = 7.8 Hz, 1H), 6.94 – 6.84 (m, 3H), 6.77 (d, *J* = 7.5 Hz, 1H), 6.73 (s, 1H).

6-Amino-2-(dicyanomethylene)-4-(4-fluorophenyl)-1,2-dihydropyridine-3,5-dicarbonitrile (17a). Yellow solid; Mp: 324-326 °C; IR (KBr): υ (cm^{-1}) = 3449, 3374, 3309, 3216, 2212, 2194, 2171, 1646. ^{1}H NMR (600 MHz, DMSO-d_6) δ 7.51 – 7.45 (m, 2H), 7.34 (t, *J* = 8.6 Hz, 2H), 6.97 (s, 2H).

4,4',4''-(((1,3,5-Triazine-2,4,6-triyl)tris(oxy))tris(benzene-4,1-diyl))tris(6-amino-2-(dicyanomethylene)-1,2-dihydropyridine-3,5-dicarbonitrile) (18a). Yellow solid; Mp: >350 °C; IR (KBr): υ (cm^{-1}) = 3504, 3374, 3224, 2215, 2194, 2166, 1613, 1551. ^{1}H NMR (400 MHz, DMSO-d_6) δ 7.53 (td, *J* = 8.5, 4.3 Hz, 1H), 7.49 – 7.41 (m, 2H), 7.38 (d, *J* = 8.6 Hz, 1H), 6.95 (s, 1H), 6.91 (s, 1H). ^{13}C NMR (101 MHz, DMSO-d_6) δ 173.3, 163.2, 159.2, 159.1, 153.2, 152.5, 133.9, 132.5, 130.6, 130.1, 122.0, 121.7, 120.6, 117.3, 117.0, 85.5, 80.8, 40.5, 40.3, 40.1.

4,4'-(1,4-Phenylene)bis(6-amino-2-(dicyanomethylene)-1,2-dihydropyridine-3,5-dicarbonitrile) (19a). Yellow solid; Mp: >350 °C; IR (KBr): υ (cm^{-1}) = 3395, 3334, 3228, 2192, 2158, 1650, 1549, 1429. ^{1}H NMR (400 MHz, DMSO-d_6) δ 7.55 (s, 1H), 6.94 (s, 1H). ^{13}C NMR (101 MHz, DMSO-d_6) δ 159.2, 144.3, 139.6, 135.2, 135.0, 134.8, 132.4, 131.5, 129.1, 128.9, 126.5, 126.4, 121.7, 121.2, 120.1, 119.6, 118.4, 116.8, 111.1, 111.0, 110.8, 102.8, 42.3.

Author information

Corresponding Author * namat@basu.ac.ir , nematollahid@gmail.com

28

424   ORCID: Davood Nematollahi: 0000-0001-9638-224X

425   **Author contributions statement**

426   A.M.N., S.B. and M.Z.: methodology, validation, investigation, writing the original draft. M.A.Z.: supervision,

427   resources, project administration, funding acquisition, conceptualization, writing-review. D.N. and S.A. writing-

428   review & editing, supervision, project administration. J.A. and H.S. did some electrochemical experiments and

429   discussions.

430   **Additional information**

431   *Supplementary information* including FT-IR, ^{1}H NMR, ^{13}C NMR, MS spectra of all new compounds accompanies this

432   paper at http://www.nature.com/srep

433   **Competing financial interests:** The authors declare no competing financial and non-financial interests

434   **References**

435   1   Makal, T. A., Li, J.-R., Lu, W. & Zhou, H.-C. Methane storage in advanced porous materials. *Chem. Soc. Rev.*
436   **41**, 7761-7779 (2012).

437   2   Davis, M. E. Ordered porous materials for emerging applications. *Nature* **417**, 813-821 (2002).

438   3   Ariga, K., Ito, H., Hill, J. P. & Tsukube, H. Molecular recognition: from solution science to nano/materials
439   technology. *Chem. Soc. Rev.* **41**, 5800-5835 (2012).

440   4   Yamauchi, Y., Suzuki, N., Radhakrishnan, L. & Wang, L. Breakthrough and future: nanoscale controls of
441   compositions, morphologies, and mesochannel orientations toward advanced mesoporous materials.
442   *Chem. Rec.* **9**, 321-339 (2009).

443   5   Fujie, K. & Kitagawa, H. Ionic liquid transported into metal–organic frameworks. *Coord. Chem. Rev.* **307**,
444   382-390 (2016).

445   6   Sarker, M., An, H. J., Yoo, D. K. & Jhung, S. H. Nitrogen-doped porous carbon from ionic liquid@ Al-metal-
446   organic framework: A prominent adsorbent for purification of both aqueous and non-aqueous solutions.
447   *Chem. Eng. J.* **338**, 107-116 (2018).

448   7   Cavka, J. H. *et al.* A New Zirconium Inorganic Building Brick Forming Metal Organic Frameworks with
449   Exceptional Stability. *J. Am. Chem. Soc.* **130**, 13850-13851 (2008).

450 8   Li, M., Li, D., O'Keeffe, M. & Yaghi, O. M. Topological analysis of metal–organic frameworks with polytopic
451   linkers and/or multiple building units and the minimal transitivity principle. *Chem. Rev.* **114**, 1343-1370
452   (2014).

453 9   Bai, Y. *et al.* Zr-based metal–organic frameworks: design, synthesis, structure, and applications. *Chem. Soc.*
454   *Rev.* **45**, 2327-2367 (2016).

455 10   Schaate, A. *et al.* Modulated synthesis of Zr-based metal–organic frameworks: from nano to single
456   crystals. *Chem.-Eur. J.* **17**, 6643-6651 (2011).

457 11   Bueken, B. *et al.* A zirconium squarate metal–organic framework with modulator-dependent molecular
458   sieving properties. *Chem. Commun.* **50**, 10055-10058 (2014).

459 12   Wang, H. *et al.* Topologically guided tuning of Zr-MOF pore structures for highly selective separation of C6
460   alkane isomers. *Nat. Commun.* **9**, 1-11 (2018).

461 13   Waitschat, S. *et al.* Synthesis of M-UiO-66 (M= Zr, Ce or Hf) employing 2, 5-pyridinedicarboxylic acid as a
462   linker: defect chemistry, framework hydrophilisation and sorption properties. *Dalton Trans.* **47**, 1062-1070
463   (2018).

464 14   Zolfigol, M. A., Khakyzadeh, V., Shirmardi, B., Moosavi-Zare, A. R. & Zare, A. Ionic liquid 3-methyl-1-
465   sulfonic acid imidazolium chloride ([Msim]Cl): A new and highly efficient catalyst for the synthesis of 1–1,
466   8-dioxo-decahydroacridine derivatives with antibacterial properties. *Clin. Biochem.* **13**, S55 (2011).

467 15   Zarei, M. Spotlight:[Msim] X: As a versatile catalyst and reagent. *Iran. J. Catal.* **8**, 237-240 (2018).

468 16   Moosavi-Zare, A. R. *et al.* Design, characterization and application of new ionic liquid 1-sulfopyridinium
469   chloride as an efficient catalyst for tandem Knoevenagel–Michael reaction of 3-methyl-1-phenyl-1*H*-
470   pyrazol-5 (4*H*)-one with aldehydes. *Appl. Catal. A* **467**, 61-68 (2013).

471 17   Babaee, S., Zolfigol, M. A., Zarei, M., Abbasi, M. & Najafi, Z. Synthesis of pyridinium-based salts: Catalytic
472   application at the synthesis of six membered *O*-heterocycles. *Mol. Catal.* **475**, 110403 (2019).

473 18   Moosavi-Zare, A. R., Zolfigol, M. A., Zarei, M., Noroozizadeh, E. & Beyzavi, M. H. Nitration of arenes by 1-
474   sulfopyridinium nitrate as an ionic liquid and reagent by in situ generation of NO_2. *RSC Adv.* **6**, 89572-
475   89577 (2016).

476 19   Moradi, S. *et al.* An efficient catalytic method for the synthesis of pyrido [2, 3-*d*] pyrimidines as biologically
477   drug candidates by using novel magnetic nanoparticles as a reusable catalyst. *Appl. Organomet. Chem.* **32**,
478   e4043 (2018).

479 20   Babaee, S., Zolfigol, M. A., Zarei, M. & Zamanian, J. 1, 10-Phenanthroline-Based Molten Salt as a
480   Bifunctional Sulfonic Acid Catalyst: Application to the Synthesis of *N*-Heterocycle Compounds via
481   Anomeric Based Oxidation. *ChemistrySelect* **3**, 8947-8954 (2018).

482 21   Pedrosa, L. F. *et al.* Synthesis and characterization of new 1*H*-pyrazolo [3, 4-*b*] pyridine phosphoramidate
483   derivatives. *Arkivoc* **4**, 38-50 (2014).

484 22   Kumar, V., Kaur, K., Gupta, G. K. & Sharma, A. K. Pyrazole containing natural products: synthetic preview
485   and biological significance. *Eur. J. Med. Chem.* **69**, 735-753 (2013).

30

486   23   Shi, D. Q., Yao, H. & Shi, J. W. Three-Component, One-Pot Synthesis of Pyrazolo [3, 4-*b*] pyridine
487   Derivatives in Aqueous Media. *Synth. Commun.* **38**, 1662-1669 (2008).

488   24   Eissa, I. H., El-Naggar, A. M. & El-Hashash, M. A. Design, synthesis, molecular modeling and biological
489   evaluation of novel 1H-pyrazolo [3, 4-*b*] pyridine derivatives as potential anticancer agents. *Bioorg. Chem.*
490   **67**, 43-56 (2016).

491   25   El-Emary, T. I. Synthesis of Newly Substituted Pyrazoles and Substituted Pyrazolo [3, 4-*b*] Pyridines Based
492   on 5-Amino-3-Methyl-1-Phenylpyrazole. *J. Chin. Chem. Soc.* **54**, 507-518 (2007).

493   26   Zhang, X. *et al.* Controllable Synthesis of Pyrazolo [3, 4-*b*] pyridines or Substituted Malononitrile
494   Derivatives through Multi-Component Reactions in Ionic Liquid. *Aust. J. Chem.* **62**, 382-388 (2009).

495   27   Afsar, J. *et al.* Synthesis and application of a novel nanomagnetic catalyst with Cl[DABCO-NO$_2$]C(NO$_2$)$_3$ tags
496   in the preparation of pyrazolo [3, 4-*b*] pyridines via anomeric based oxidation. *Res. Chem. Intermed.* **44**,
497   7595-7618 (2018).

498   28   Alabugin, I. V. Stereoelectronic Effects. *A Bridge Between Structure and Reactivity* (2016).

499   29   Alabugin, I. V., dos Passos Gomes, G. & Abdo, M. A. Hyperconjugation. *Wiley Interdiscip. Rev. Comput.*
500   *Mol. Sci* **9**, e1389 (2019).

501   30   Yarie, M. Spotlight: Catalytic vinylogous anomeric based oxidation (Part I). *Iran. J. Catal* **10**, 79-83 (2020).

502   31   Yarie, M. Catalytic anomeric based oxidation. *Iranian Journal of Catalysis Spotlight* **7**, 85-88 (2017).

503   32   Karimi, F., Yarie, M. & Zolfigol, M. A. Synthesis and characterization of Fe$_3$O$_4$@
504   SiO$_2$@(CH$_2$)$_3$NH(CH$_2$)$_2$O$_2$P(OH)$_2$ and its catalytic application in the synthesis of benzo-[*h*] quinoline-4-
505   carboxylic acids via a cooperative anomeric based oxidation mechanism. *Mol. Catal.* **489**, 110924 (2020).

506   33   Afsar, J. *et al.* Synthesis and application of melamine-based nano catalyst with phosphonic acid tags in the
507   synthesis of (3´-indolyl) pyrazolo [3, 4-*b*] pyridines via vinylogous anomeric based oxidation. *Mol. Catal.*
508   **482**, 110666 (2020).

509   34   Babaee, S., Zarei, M., Sepehrmansourie, H., Zolfigol, M. A. & Rostamnia, S. Synthesis of Metal–Organic
510   Frameworks MIL-101(Cr)-NH$_2$ Containing Phosphorous Acid Functional Groups: Application for the
511   Synthesis of *N*-Amino-2-pyridone and Pyrano [2, 3-*c*] pyrazole Derivatives via a Cooperative Vinylogous
512   Anomeric-Based Oxidation. *ACS omega* **5**, 6240-6249 (2020).

513   35   Jalili, F., Zarei, M., Zolfigol, M. A., Rostamnia, S. & Moosavi-Zare, A. R. SBA-15/PrN(CH$_2$PO$_3$H$_2$)$_2$ as a novel
514   and efficient mesoporous solid acid catalyst with phosphorous acid tags and its application on the
515   synthesis of new pyrimido [4, 5-*b*] quinolones and pyrido [2, 3-*d*] pyrimidines via anomeric based
516   oxidation. *Micropor. Mesopor. MAT.* **294**, 109865 (2020).

517   36   Ghasemi, P., Yarie, M., Zolfigol, M. A., Taherpour, A. A. & Torabi, M. Ionically Tagged Magnetic
518   Nanoparticles with Urea Linkers: Application for Preparation of 2-Aryl-quinoline-4-carboxylic Acids via an
519   Anomeric-Based Oxidation Mechanism. *ACS omega* **5**, 3207-3217 (2020).

520   37   Karimi, F., Yarie, M. & Zolfigol, M. A. A convenient method for synthesis of terpyridines via a cooperative
521   vinylogous anomeric based oxidation. *RSC Adv.* **10**, 25828-25835 (2020).

31

522 38 Dashteh, M. *et al.* Synthesis of cobalt tetra-2, 3-pyridiniumporphyrazinato with sulfonic acid tags as an
523 efficient catalyst and its application for the synthesis of bicyclic ortho-aminocarbonitriles, cyclohexa-1, 3-
524 dienamines and 2-amino-3-cyanopyridines. *RSC Adv.* **10**, 27824-27834 (2020).

525 39 Alizadeh, S. & Nematollahi, D. Electrochemically assisted self-assembly technique for the fabrication of
526 mesoporous metal–organic framework thin films: composition of 3D hexagonally packed crystals with 2D
527 honeycomb-like mesopores. *J. Am. Chem. Soc.* **139**, 4753-4761 (2017).

528 40 Alizadeh, S. & Nematollahi, D. convergent and Divergent paired electrodeposition of Metal-organic
529 framework thin films. *Sci. Rep.* **9**, 1-13 (2019).

530 41 Wagner, A. Preparation, functionalization and analysis of UiO-66 metal-organic framework thin films on
531 silicon photocathodes. *Uppsala University* (2015).

532 42 Li, M. & Dincă, M. On the Mechanism of MOF-5 Formation under Cathodic Bias. *Chem. Mater.* **27**, 3203-
533 3206 (2015).

534 43 Li, M. & Dinca, M. Reductive electrosynthesis of crystalline metal–organic frameworks. *J. Am. Chem. Soc.*
535 **133**, 12926-12929 (2011).

536 44 Campagnol, N. *et al.* On the electrochemical deposition of metal–organic frameworks. *J. Mater. Chem. A.*
537 **4**, 3914-3925 (2016).

538 45 Soury, S., Bahrami, A., Alizadeh, S., Shahna, F. G. & Nematollahi, D. Development of a needle trap device
539 packed with zinc based metal-organic framework sorbent for the sampling and analysis of polycyclic
540 aromatic hydrocarbons in the air. *Microchem. J.* **148**, 346-354 (2019).

541 46 Firoozichahak, A. *et al.* UIO-66-NH$_2$ Packed Needle Trap for Accurate and Reliable Sampling and Analysis of
542 the Halogenated Volatile Organic Compounds in Air. *Int. J. Environ. Anal. Chem.*, 1-18 (2019).

543 47 Firoozichahak, A. *et al.* Development of a needle trap device packed with titanium based metal-organic
544 framework sorbent for extraction of phenolic derivatives in air. *J. Sep. Sci.* (2019).

545 48 Pirmohammadi, Z. *et al.* Determination of urinary methylhippuric acids using MIL-53-NH$_2$ (Al) metal–
546 organic framework in microextraction by packed sorbent followed by HPLC–UV analysis. *Biomed.*
547 *Chromatogr.* **34**, e4725 (2020).

548 49 Saedi, N. *et al.* A needle trap device packed with MIL-100 (Fe) metal organic frameworks for efficient
549 headspace sampling and analysis of urinary BTEXs. *Biomed. Chromatogr.* **34**, e4800 (2020).

550 50 Langari, A. A. A., Firoozichahak, A., Alizadeh, S., Nematollahi, D. & Farhadian, M. Efficient extraction of
551 aromatic amines in the air by the needle trap device packed with the zirconium based metal–organic
552 framework sorbent. *RSC. Adv.* **10**, 13562-13572 (2020).

553 51 DeStefano, M. R., Islamoglu, T., Garibay, S. J., Hupp, J. T. & Farha, O. K. Room-temperature synthesis of
554 UiO-66 and thermal modulation of densities of defect sites. *Chem. Mater.* **29**, 1357-1361 (2017).

555 52 Shearer, G. C. *et al.* Defect engineering: tuning the porosity and composition of the metal–organic
556 framework UiO-66 via modulated synthesis. *Chem. Mater.* **28**, 3749-3761 (2016).

557　53　Trickett, C. A. *et al.* Definitive molecular level characterization of defects in UiO-66 crystals. *Angew. Chem.,*
558　　　*Int. Ed.* **54**, 11162-11167 (2015).

559　54　Stassen, I. *et al.* Electrochemical film deposition of the zirconium metal–organic framework UiO-66 and
560　　　application in a miniaturized sorbent trap. *Chem. Mater.* **27**, 1801-1807 (2015).

561　55　Wei, J.-Z. *et al.* Rapid and low-cost electrochemical synthesis of UiO-66-NH$_2$ with enhanced fluorescence
562　　　detection performance. *Inorg. Chem.* **58**, 6742-6747 (2019).

563　56　Zhang, T. *et al.* Rapid synthesis of UiO-66 by means of electrochemical cathode method with
564　　　electrochemical detection of 2, 4, 6-TCP. *Inorg. Chem. Commun.* **111**, 107671 (2020).

565　57　Momeni, S. & Nematollahi, D. New insights into the electrochemical behavior of acid orange 7:
566　　　Convergent paired electrochemical synthesis of new aminonaphthol derivatives. *Sci. Rep.* **7**, 1-10 (2017).

567　58　Mokhtari, B., Nematollahi, D. & Salehzadeh, H. Paired electrochemical conversion of nitroarenes to
568　　　sulfonamides, diarylsulfones and bis (arylsulfonyl) aminophenols. *Green Chem.* **20**, 1499-1505 (2018).

569　59　Jamshidi, M., Nematollahi, D., Taheri, F. & Alizadeh, H. Paired Electrochemical Method for Synthesis of
570　　　New Phenylcarbonimidoyl Dicyanide Dyes. *Acs. Sustain. Chem.Eng.* **7**, 1956-1962 (2018).

571　60　Amatore, C. & Brown, A. R. Paired electrosynthesis at the femtoliter scale: formation of 9, 10-
572　　　Anthracenedione from the oxidation of Anthracene and reduction of dioxygen. *J. Am. Chem. Soc.* **118**,
573　　　1482-1486 (1996).

574　61　Frontana-Uribe, B. A., Little, R. D., Ibanez, J. G., Palma, A. & Vasquez-Medrano, R. Organic
575　　　electrosynthesis: a promising green methodology in organic chemistry. *Green. Chem.* **12**, 2099-2119
576　　　(2010).

577　62　Llorente, M. J., Nguyen, B. H., Kubiak, C. P. & Moeller, K. D. Paired electrolysis in the simultaneous
578　　　production of synthetic intermediates and substrates. *J. Am. Chem. Soc.* **138**, 15110-15113 (2016).

579　63　Wu, T., Nguyen, B. H., Daugherty, M. C. & Moeller, K. D. Paired Electrochemical Reactions and the On-Site
580　　　Generation of a Chemical Reagent. *Angew. Chem.* **131**, 3600-3603 (2019).

581　64　Fuentes, L. & JJ, V. Synthesis Of Heterocyclic Compounds. Xxiii: Pyridines From Malononitrile Dimer And
582　　　Benzylidenemalononitriles. **4**, 320-322 (1982).

583　65　Moustafa, M. S. *et al.* Unexpected behavior of enaminones: interesting new routes to 1, 6-naphthyridines,
584　　　2-oxopyrrolidines and pyrano [4, 3, 2-*de*][1, 6] naphthyridines. *Molecules* **18**, 276-286 (2013).

585　66　Katritzky, A. R., Steel, P. J. & Denisenko, S. N. X-Ray crystallographic evidence for a vinylogous anomeric
586　　　effect in benzotriazole-substituted heterocycles. *Tetrahedron* **57**, 3309-3314 (2001).
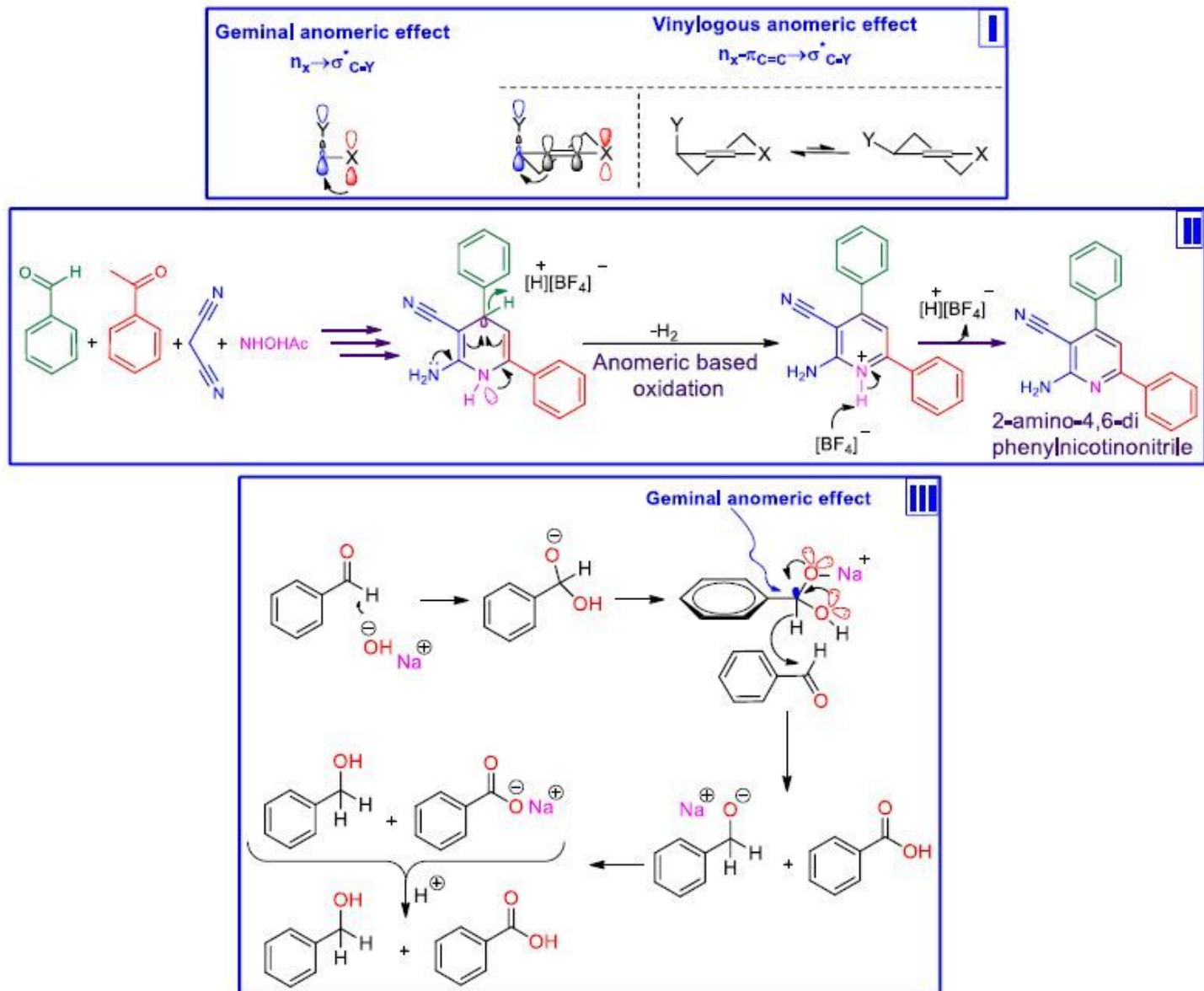
33

Figures

Figure 1

Part I: Geminal versus vinylogous anomeric effect. Part II: A cooperative vinylogous anomeric based oxidation leads to the preparation of 2-amino-4,6-diphenylnicotinonitrile 30. Part III: A cooperative germinal anomeric based oxidation leads to hydride transfer in the mechanism of Cannizzaro reaction 31 (CambridgeSoft).
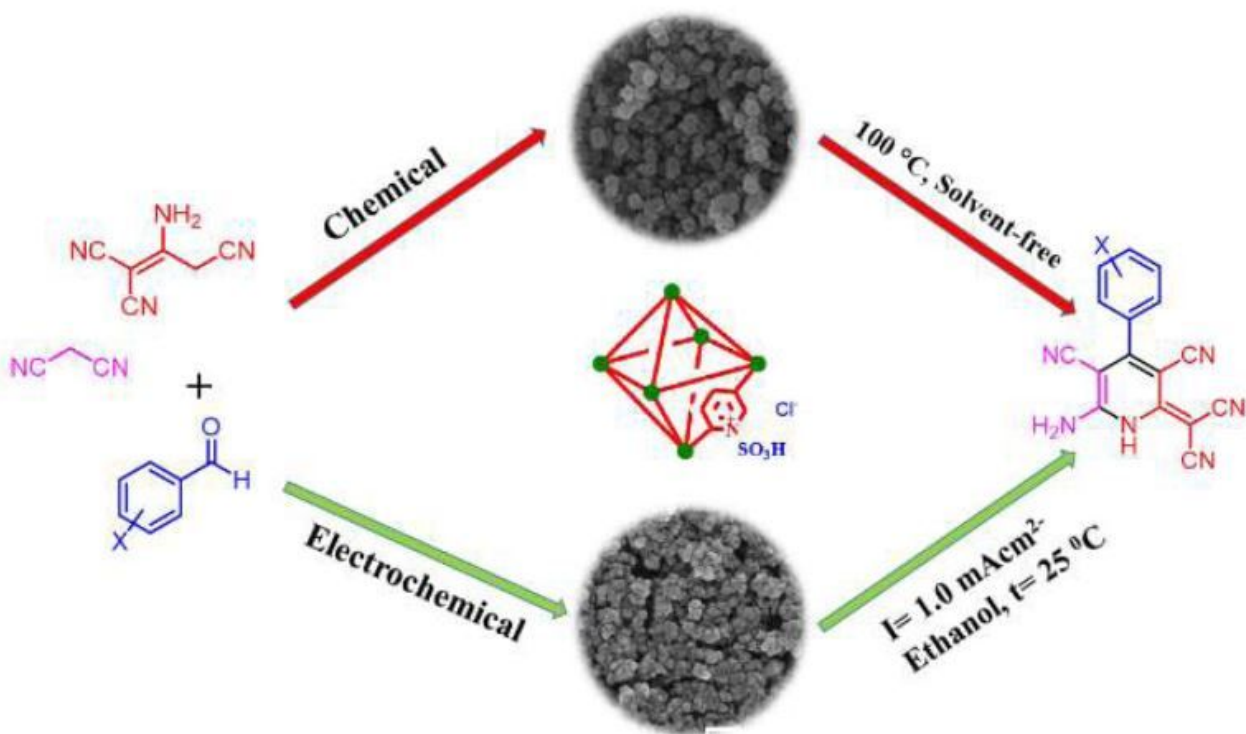
Figure 2

Synthesis of dicyanomethylene pyridines using [Zr-UiO-66-PDC-SO3H]Cl as a catalyst by chemical and electrochemical methods.
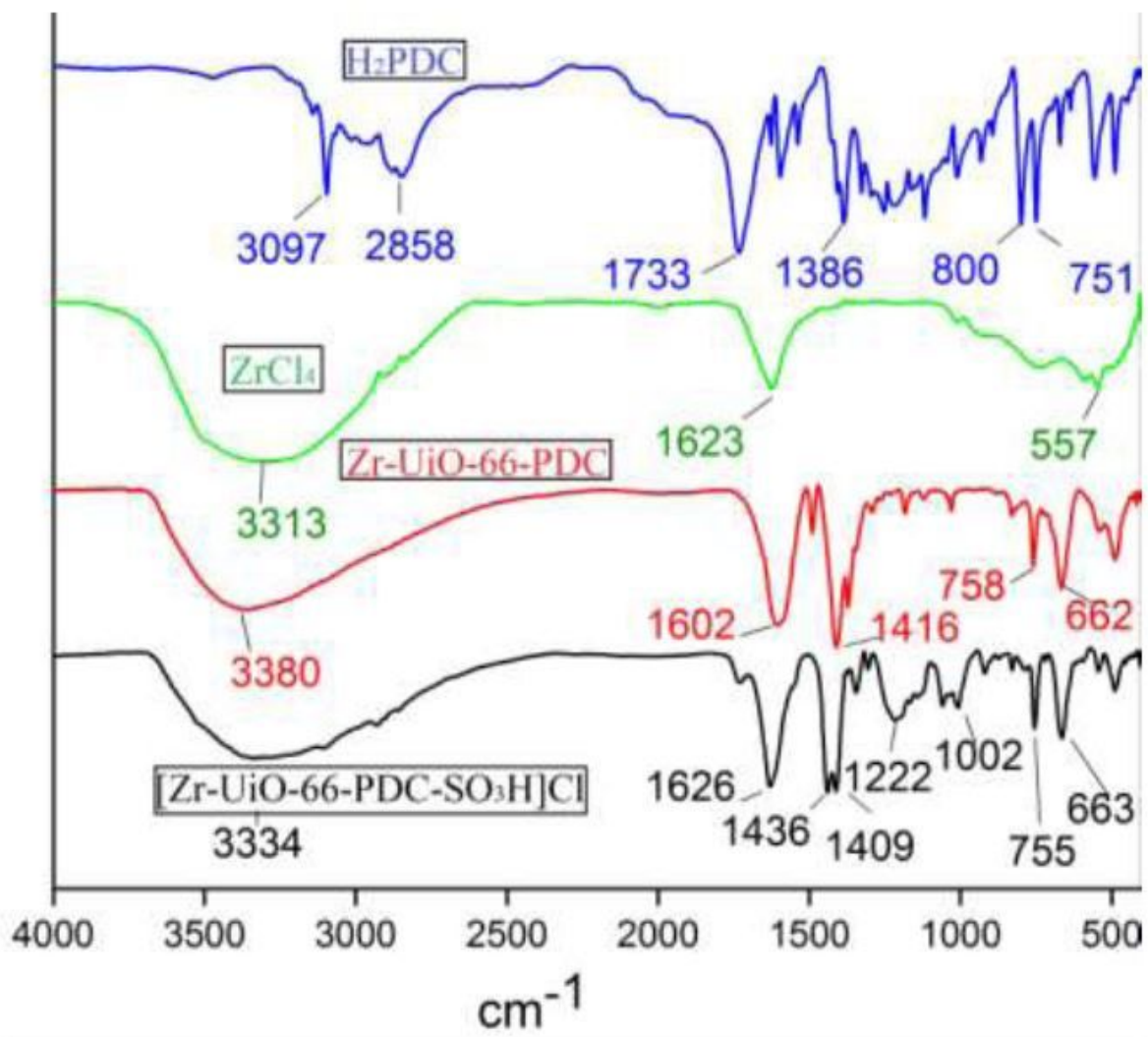
Figure 3

FT-IR spectrum of pyridine-2,5-dicarboxylic acid (H2PDC), ZrCl4, Zr-UiO-66-PDC and [Zr-UiO-66-PDC-SO3H]Cl.
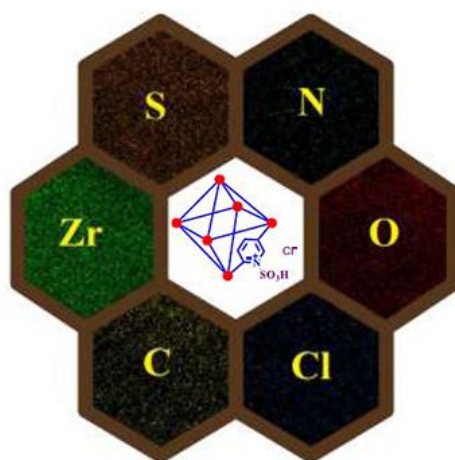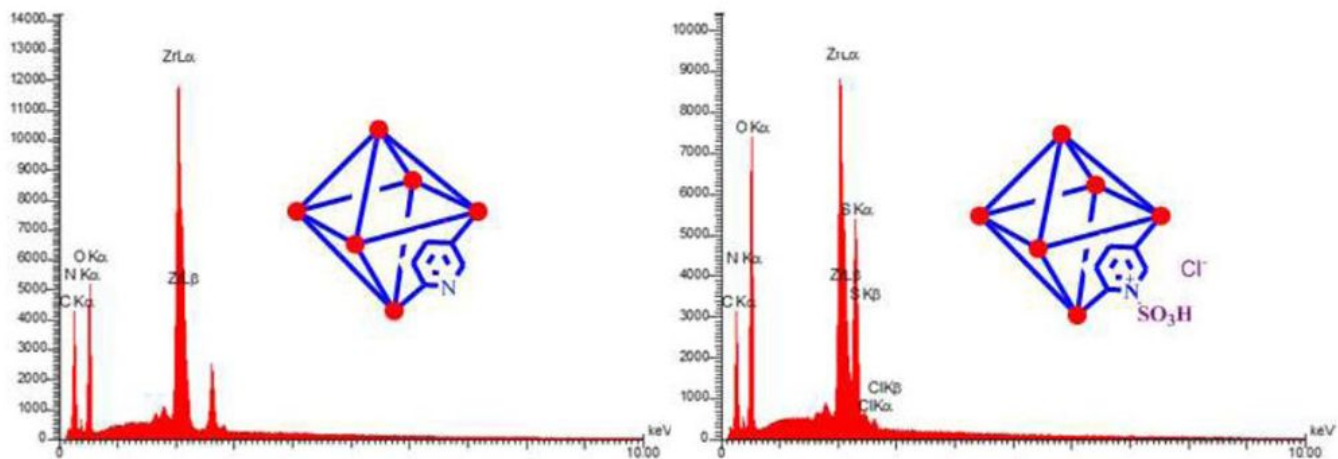
Figure 4

Up: Energy-dispersive X-ray spectroscopy (EDX) of [Zr-UiO-66-PDC-SO3H]Cl and Zr-UiO-66-PDC. Down: Elemental mapping analysis of [Zr-UiO-66-PDC-SO3H]Cl. The structures of the compounds were drawn using ChemOffice 12.0 (CambridgeSoft).
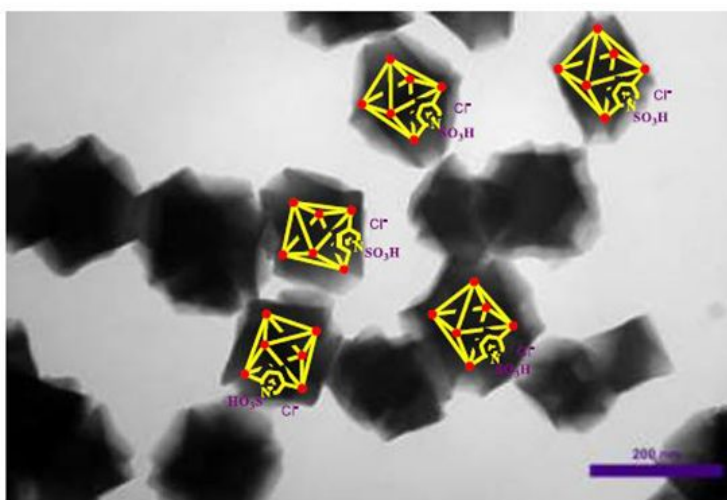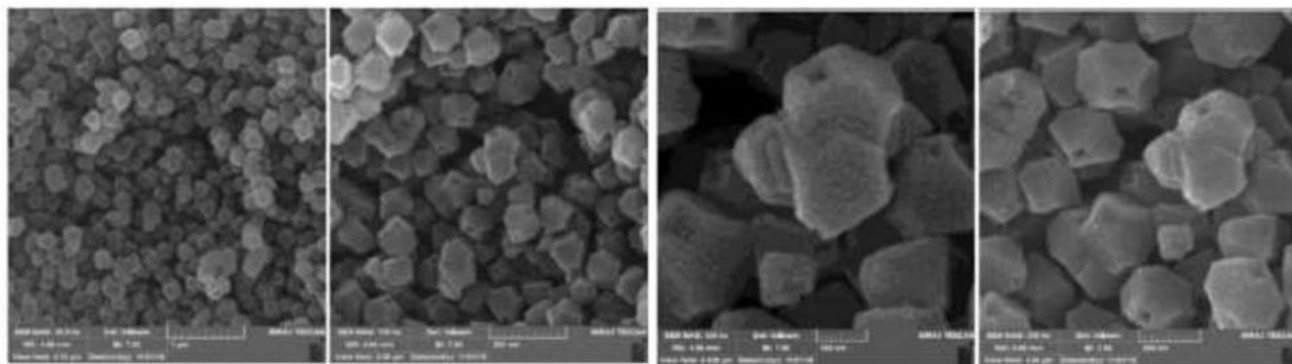
Figure 5

Up: Scanning electron microscopy (SEM) images of [Zr-UiO-66-PDC-SO3H]Cl. Down: Transmission electron microscopy (TEM) micrograph of [Zr-UiO-66-PDC-SO3H]Cl.
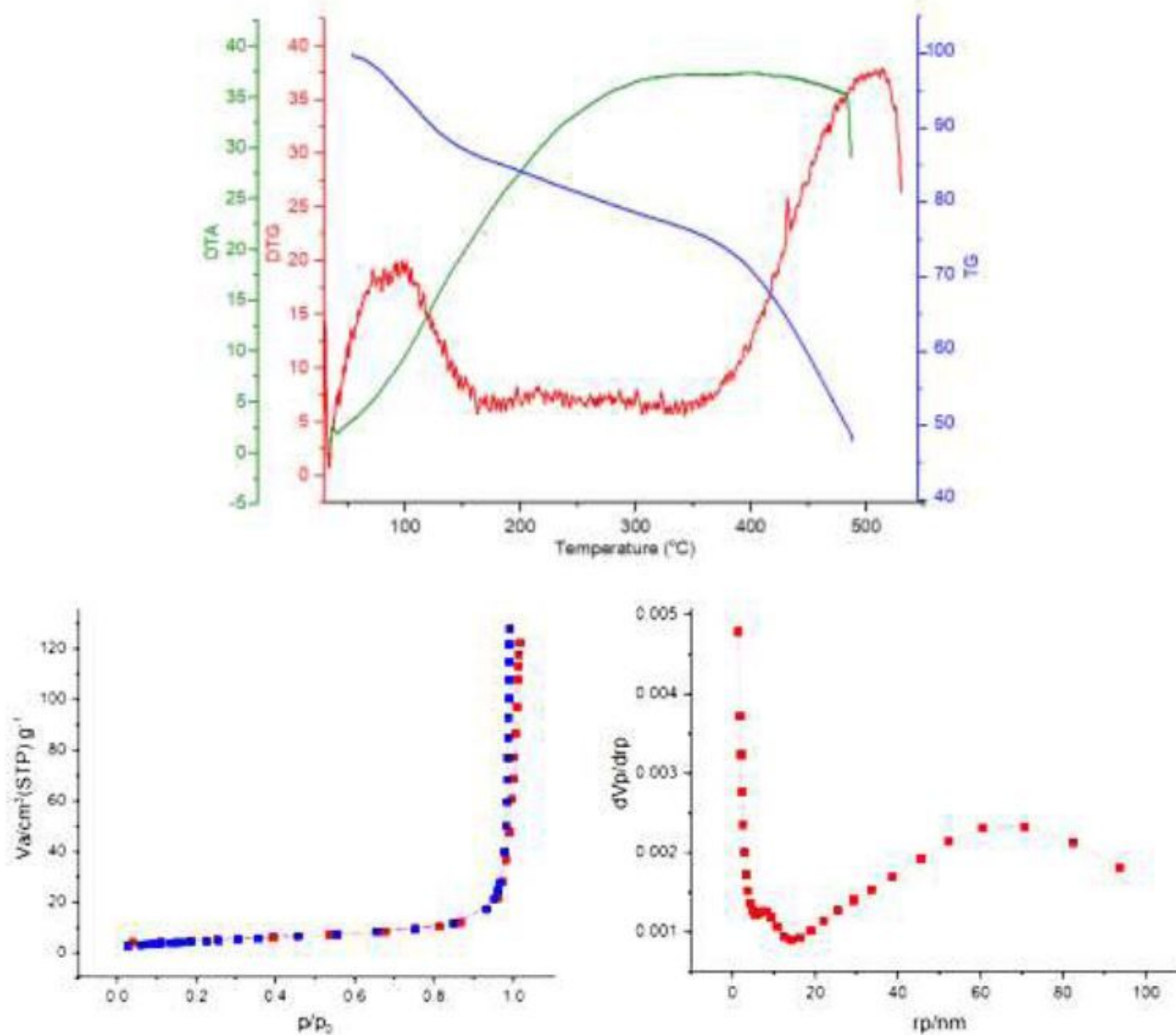
Figure 6

Up: TG, DTG and DTA analysis of [Zr-UiO-66-PDC-SO3H]Cl. This figure was prepared by Microsoft Excel (OFFICE 2013). Down: N2 adsorption/desorption isotherm and pore size distribution (BJH) of [Zr-UiO-66-PDC-SO3H]Cl. This figure was prepared by Microsoft Excel (OFFICE 2013).
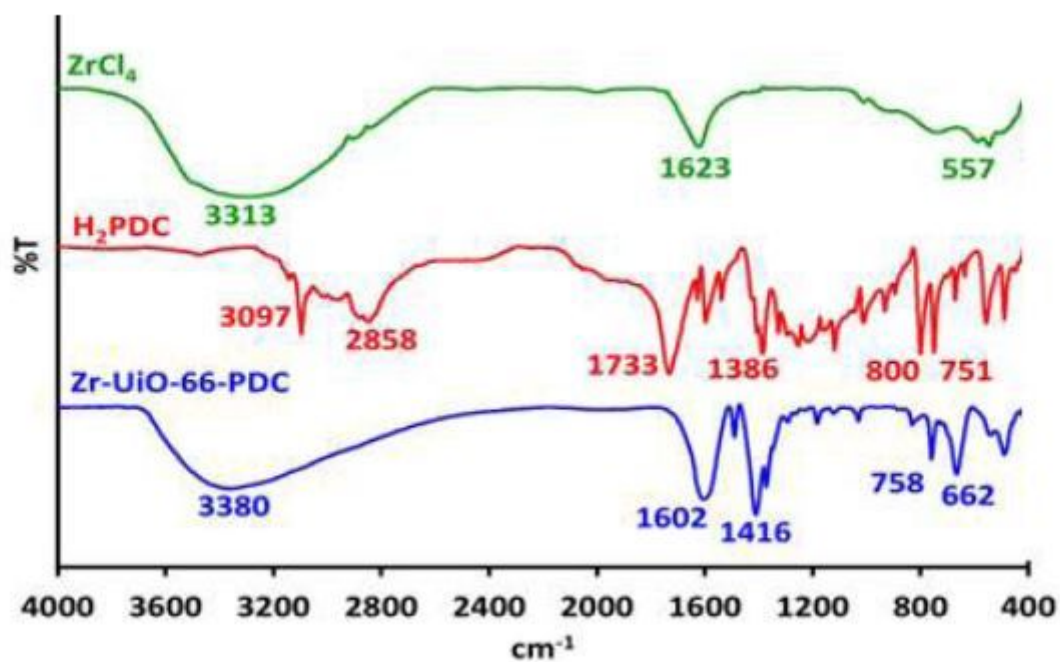
Figure 7

Up: Electrochemical synthesis of (UiO-66-PDC) by constant current electrolysis at I = 30 mA cm-2 and t = 1800 s. Down: Comparison of FT-IR spectra of pyridine-2,5-dicarboxylic acid (H2PDC), ZrCl4 and Zr-UiO-66-PDC. The structures of the compounds were drawn using ChemOffice 12.0 (CambridgeSoft).
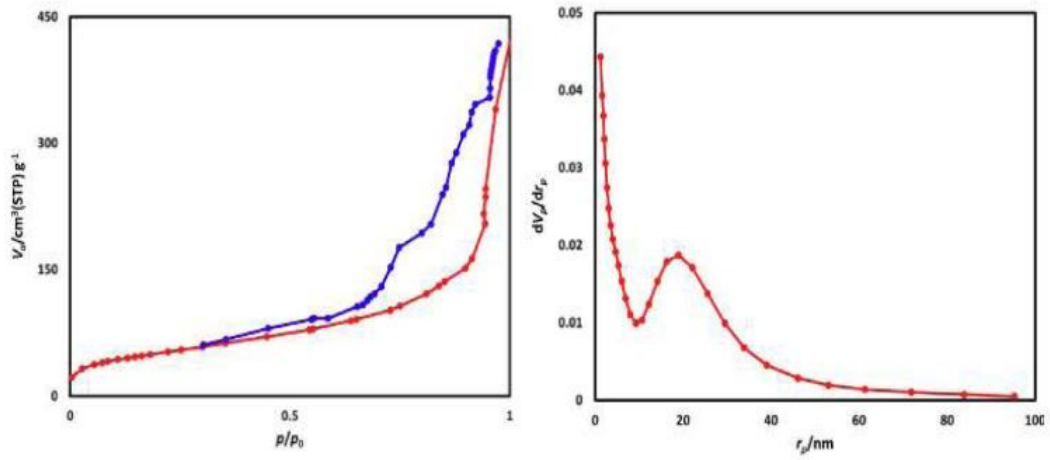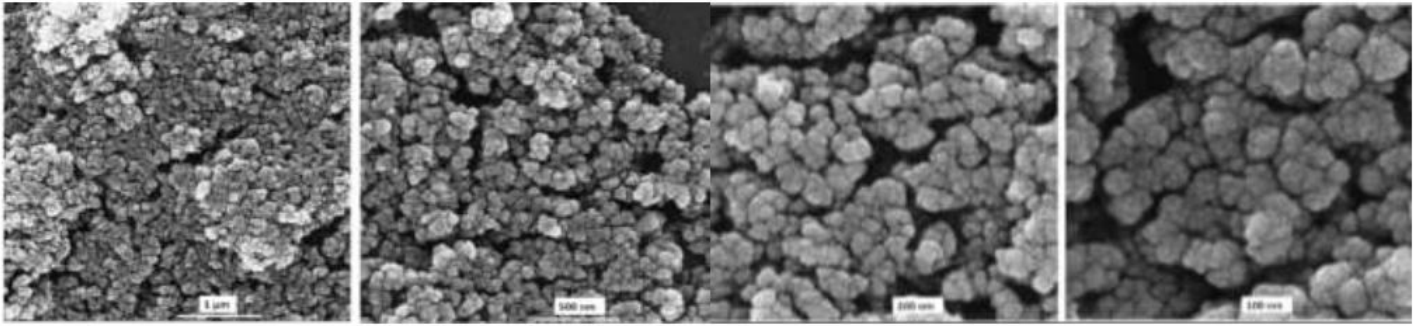
Figure 8

Up: Large- and close-view FE-SEM images of Zr-UiO-66-PDC by constant current electrolysis at I= 30 mA cm-2 and t = 1800 s. Down: N2 adsorption/desorption isotherm. BET and BJH of Zr-UiO-66-PDC by the constant current electrolysis at I= 30 mA cm-2 and t = 1800 s.
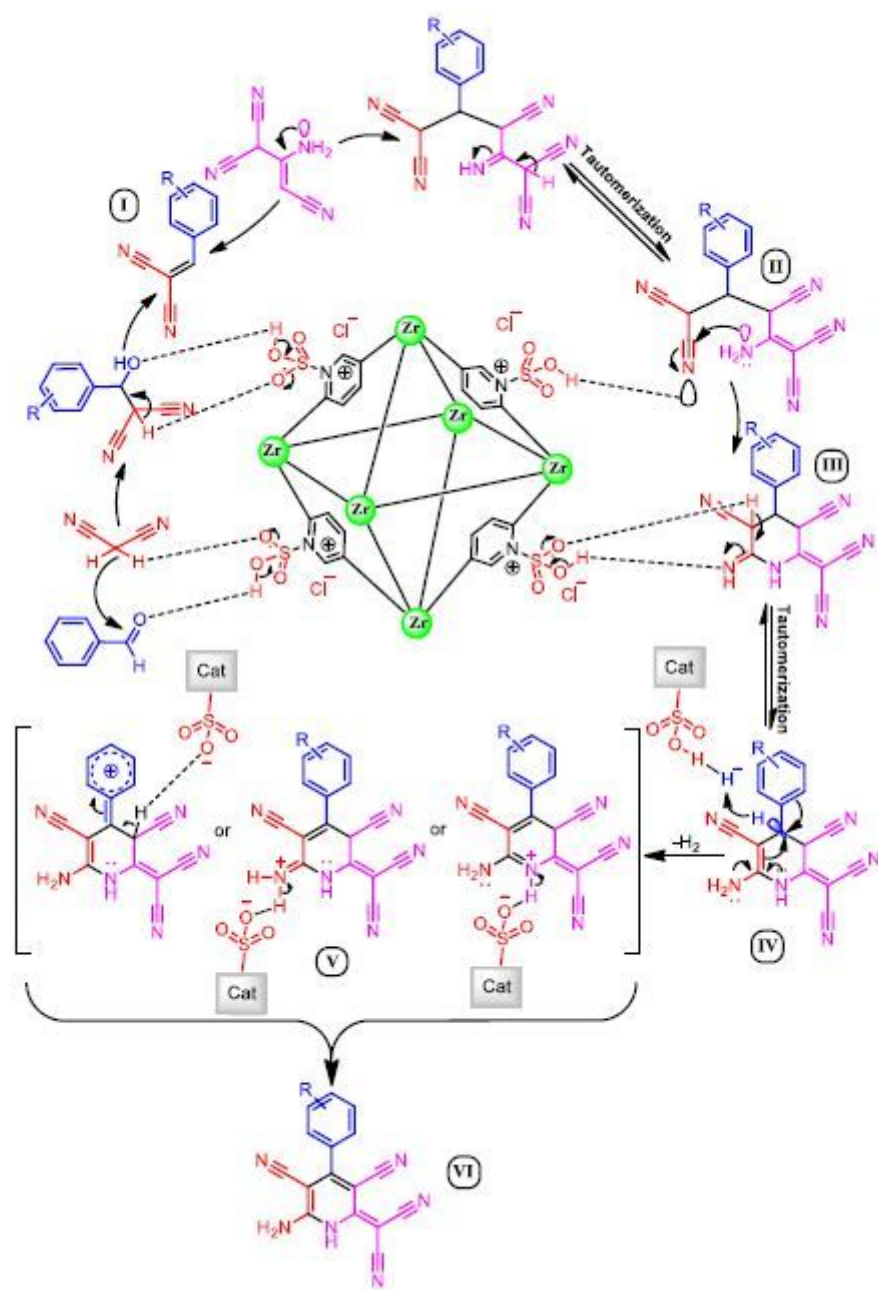
Figure 9

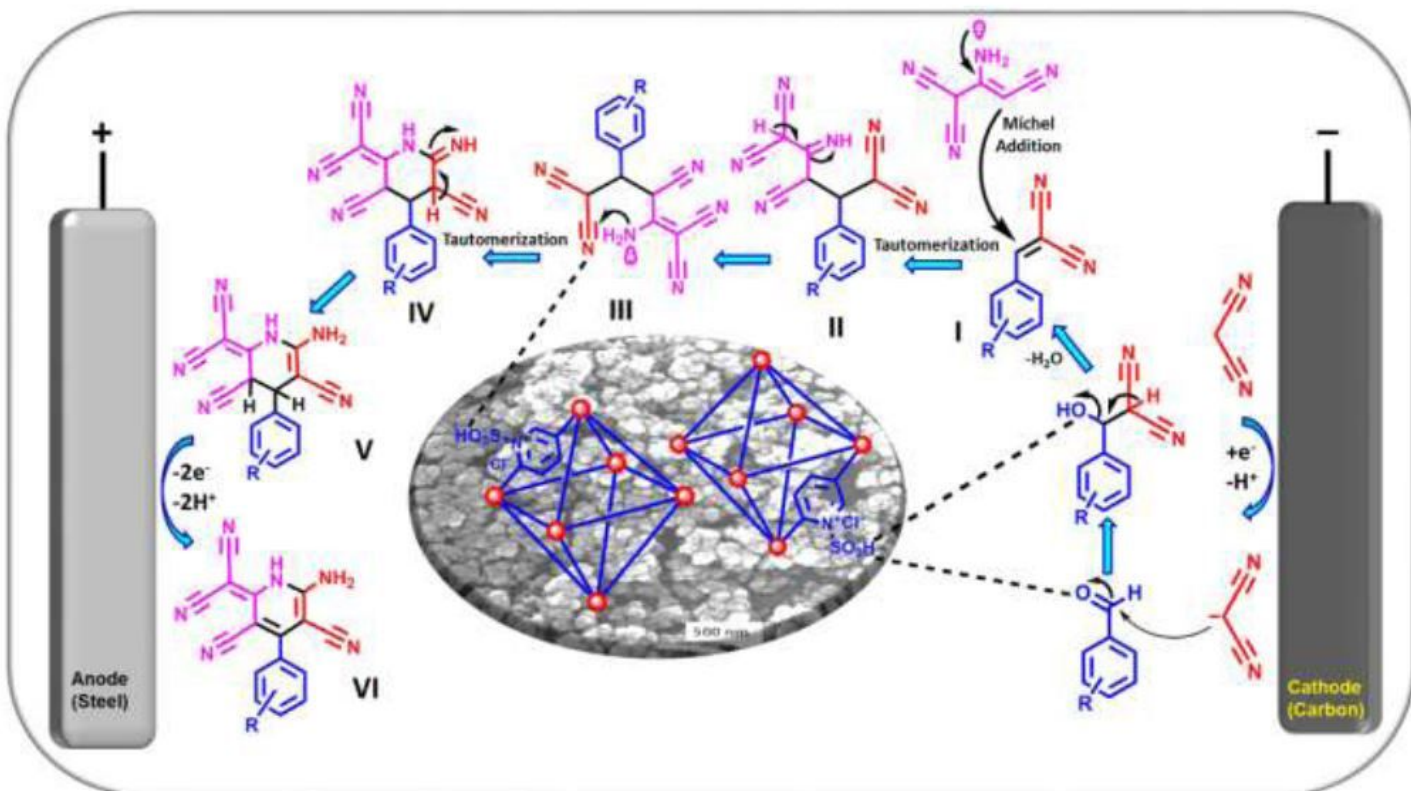A rational proposed mechanism for the synthesis of dicyanomethylene pyridine using [Zr-UiO-66-PDC-SO3H]Cl.

Figure 10

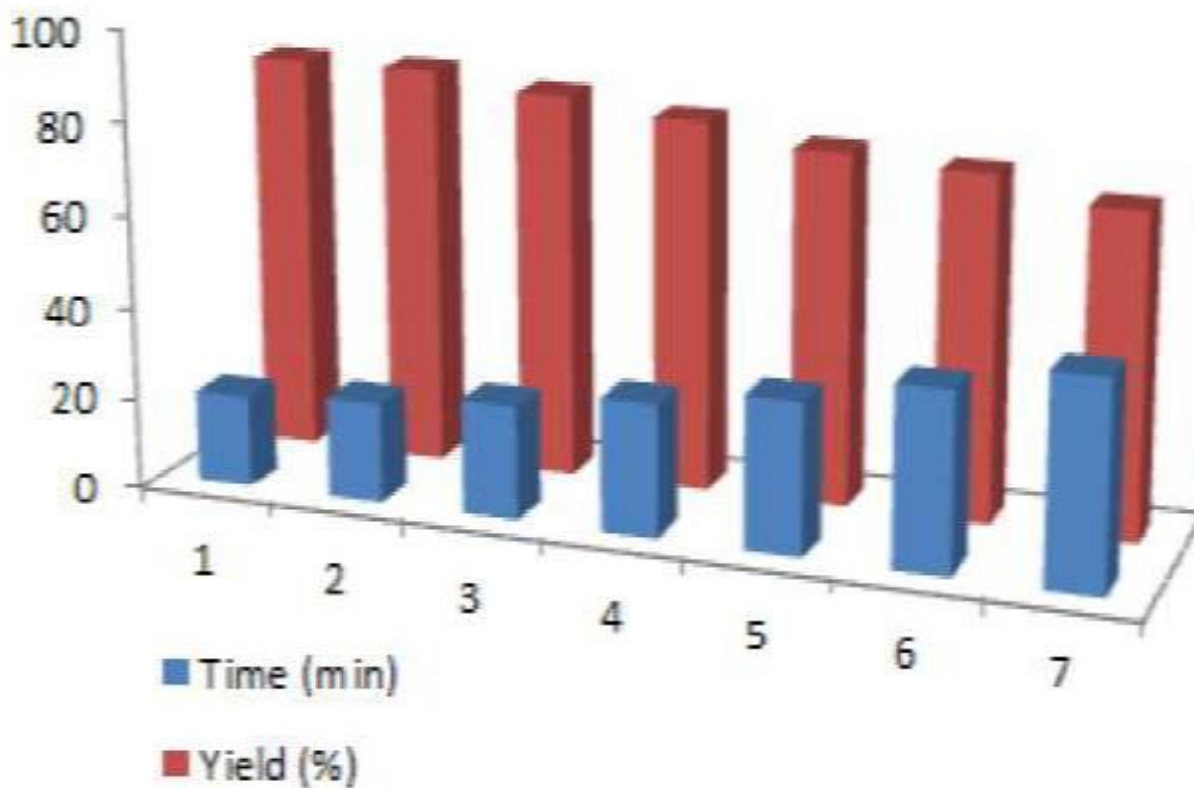Convergent paired electrochemical synthesis of dicyanomethylene pyridine compounds.

Figure 11

Recyclability of of [Zr-UiO-66-PDC-SO3H]Cl at the synthesis (2-methyl-1H-indol-3-yl)-pyrazolo[3,4-b]pyridine derivatives.
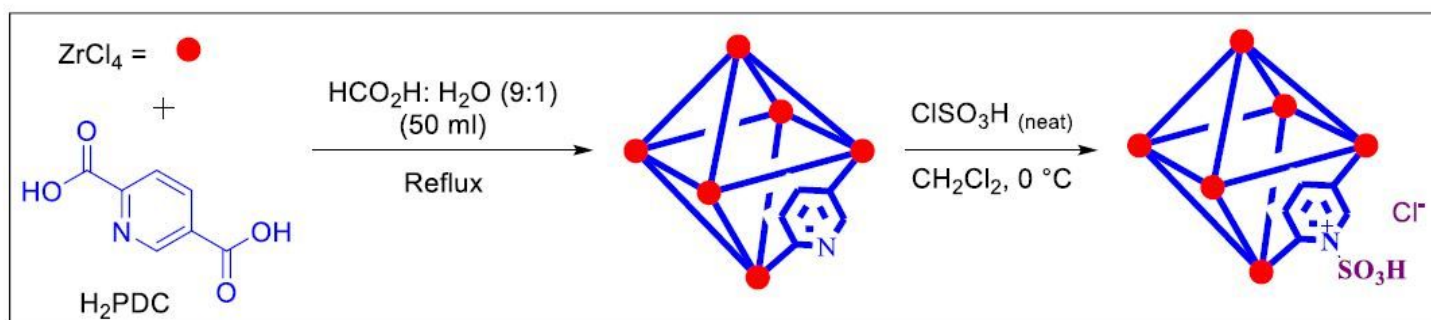

Figure 12

Chemical synthesis of [Zr-UiO-66-PDC-SO3H]Cl as a functionalized MOF catalyst

Supplementary Files

This is a list of supplementary files associated with this preprint. Click to download.

- SINematollahizolfigol.pdf